ADVANCED HEALTHCARE MATERIALS
www.advhealthmat.de

Models of the Gut for Analyzing the Impact of Food and Drugs

*Chiara Anna Maria Fois, Thi Yen Loan Le, Aaron Schindeler, Sina Naficy, Dale David McClure, Mark Norman Read, Peter Valtchev, Ali Khademhosseini, and Fariba Dehghani**

Models of the human gastrointestinal tract (GIT) can be powerful tools for examining the biological interactions of food products and pharmaceuticals. This can be done under normal healthy conditions or using models of disease–many of which have no curative therapy. This report outlines the field of gastrointestinal modeling, with a particular focus on the intestine. Traditional in vivo animal models are compared to a range of in vitro models. In vitro systems are elaborated over time, recently culminating with microfluidic intestines-on-chips (IsOC) and 3D bioengineered models. Macroscale models are also reviewed for their important contribution in the microbiota studies. Lastly, it is discussed how in silico approaches may have utility in predicting and interpreting experimental data. The various advantages and limitations of the different systems are contrasted. It is posited that only through complementary use of these models will salient research questions be able to be addressed.

1. Introduction

The human intestine is the primary organ responsible for the uptake of nutrients and water, and this is facilitated by its complex structure that features a large surface area. With an average total length of around seven meters, including both small and large intestine, it connects the stomach to the rectum while enabling absorption in a specialized manner. At a cellular level, the gut epithelium is critical in selective transport to the bloodstream. The finger-like projections of the intestinal epithelium increase the total area available for resorption. Moreover, the human intestine is naturally defended by a complex immune system which defends against undesired infiltrations through the gut, such as bacteria. Recent studies are also investigating the gut–brain axis and the role of microbiota and dysbiosis,[1] as this seems to be involved in the development of chronical diseases, inflammation, obesity, and neurodisorders.[2]

Inflammatory bowel disease (IBD), namely Crohn's disease and ulcerative colitis, can all necessitate special dietary restrictions (e.g., fermentable oligo-, di-, mono-saccharides and polyols (FODMAP), enteral nutrition, and low fibers).[3] Notably, food is seen not only as the potential and partial cause of these illnesses, but can be efficiently adopted for suppressing disease symptoms. However, such approaches are currently unreliable and rarely personalized for individual patients. It is expected that gut models will continue to have an important role in elucidating mechanisms of gut disease and developing new therapeutic approaches.

Historically, animal models have been employed to study gut disease and gastrointestinal function. While there are some concerns that gut microbiota and intestinal morphology in the rodent models can differ from the human condition,[4] they are nonetheless widely used. Still, compared to in vitro models, animal studies have a high barrier to entry in terms of expense, training, and ethical practices. Cell culture is still the basis for many in vitro models, with researchers recapitulating the natural villi morphology of the intestine using scaffold structures,[5] or recreating the mucosa layer, naturally present in the human gut using hydrogels.[6]

Advances in culture methods, particularly, in the area of microfluidics such as organs-on-chip technology,[7] have the potential to radically shift analysis methods. They are low cost with microfluidic perfusion feasible in micrometer size chambers. The use of human cells can better mimic human physiology and can also use individual patient-derived cells to model specific disease conditions. Such individualized approaches are highly relevant for personalized medicine. Intestines-on-chips (IsOC) are not a new discovery, first described over a decade ago, but advances in chip manufacturing have lowered costs and improved versatility and accessibility.

C. A. M. Fois, Dr. T. Y. L. Le, Prof. A. Schindeler, Dr. S. Naficy, Dr. D. D. McClure, Dr. M. N. Read, Dr. P. Valtchev, Prof. F. Dehghani
School of Chemical and Biomolecular Engineering
Centre for Advanced Food Enginomics
University of Sydney
Sydney, NSW 2006, Australia
E-mail: fariba.dehghani@sydney.edu.au
Prof. A. Khademhosseini
Department of Chemical and Biomolecular Engineering
Department of Bioengineering
Department of Radiology
California NanoSystems Institute (CNSI)
University of California
Los Angeles, CA 90095, USA
The ORCID identification number(s) for the author(s) of this article can be found under https://doi.org/10.1002/adhm.201900968.

DOI: 10.1002/adhm.201900968

In silico models have the potential to complement data taken from in vitro experiments, performed both in standard multiwell plates and in microfluidic systems. There is particular utility for their application in pharmacokinetics (PK) and pharmacodynamics (PD) studies where the role of the intestine in drug absorption is being increasingly appreciated.

This Progress Report aims to provide an overview of the complexities associated with the physiology of the gastrointestinal tract (GIT) and then discuss the utility of the aforementioned model systems. **Figure 1** presents a schematic representation of the classes of models to be discussed.

2. The Physiological and Pathological of the Gastrointestinal Tract

2.1. The Human Gut: Structure and Function

The human gut or GIT is a multiple organs system. Anatomically, it can be divided into the upper and lower GIT. The upper GIT comprises the mouth, esophagus, stomach, and intestines, while the lower GIT consists of the colon, rectum, and anus (Figure 1).

The GIT digests the food to extract nutrients necessary for our living. The mouth is the beginning of the GIT. After food is taken into the mouth, it is pushed down by the esophagus into the stomach via a wave-like contraction of muscles in the esophagus. The stomach lining secretes gastric acid and digestive enzymes to break down the food further and digests it. The mixture of partially digested food with enzymes in the stomach is known as "chyme." After this digestive process is complete, the chyme exits the stomach and enters the small intestine through the pyloric sphincter. The small intestine is a tube-like structure, which comprises three main segments: duodenum (first), jejunum (middle), and ileum (last). Enzymes and other excretions secreted by the gallbladder and pancreas enter the duodenum via the bile and pancreatic ducts. In the duodenum, foods are further broken down by digestive enzymes to extract nutrients (such as proteins, fats, and carbohydrates) and this is followed by intestinal absorption. The epithelial cells in the jejunum of the small intestine absorb nutrients into the bloodstream via a network of capillaries and lymphatic vessels. In contrast, absorption of water occurs in the large intestinal mucosa. Leftover products are then passed down from the small intestine into the colon through the ileocecal valve. The large intestine is responsible for solidification of the colonic contents into feces, storage, and expulsion. Additional organs that aid in the digestive process include the salivary glands, pancreas, liver, and gallbladder.

A schematic of the human gut is shown in **Figure 2**, illustrating the functional layers of the GIT including the outer serosa layer, the smooth muscle layers followed by the submucosa layer and an inner absorptive mucosa.[8] The mucosa is the inner absorptive layer of the gut which composes of the muscularis mucosae, lamina propria, and epithelium. Secretory and absorptive epithelial cells within the mucosal layer consist of pits called "crypts" that form a circle around and provide epithelial cells to projecting out finger-like structures called "villi." The jejunum portion of the small intestine is rich in villi, responsible for nutrient absorption. Next to the mucosa is the submucosal layer, which contains connective tissue, a network of capillaries, nerves, and lymphatics vessels. The contraction of the intestine is regulated by the longitudinal and circular layers smooth muscle cells, with intercalated enteric nerves regulating their contractions. During the digestive phase, these

Chiara Anna Maria Fois received both a Bachelor and a Master Degree in chemical engineering at the University of Cagliari, Italy. In 2017, she has joined Professor Fariba Dehghani's team at the Centre for Advanced Food Enginomics. She is currently pursuing a Ph.D. degree at the School of Chemical and Biomolecular Engineering, the University of Sydney. Her research focuses on microfluidics and processes downscaling with specific interest in the development of organs-on-chips for the study of food effects on human health.

Ali Khademhosseini is the Levi Knight Professor of Bioengineering, Chemical Engineering and Radiology at the University of California—Los Angeles. He is the Founding Director of the Center for Minimally Invasive Therapeutics at UCLA. His interdisciplinary group is developing "personalized" solutions that utilize micro- and nanotechnologies to enable a range of therapies for organ failure, cardiovascular disease, and cancer. In enabling this vision, he works closely with clinicians, including interventional radiologists, cardiologists, and surgeons.

Fariba Dehghani is currently the Director of Centre for Advanced Food Enginomics and a former director of the ARC Food Processing Training Centre in the School of Chemical and Biomolecular Engineering at the University of Sydney. Her research team in collaboration with industry has worked together to provide pragmatic, cost-effective, and environmentally sustainable solutions to a diverse range of issues, with the aim of improving human well-being.

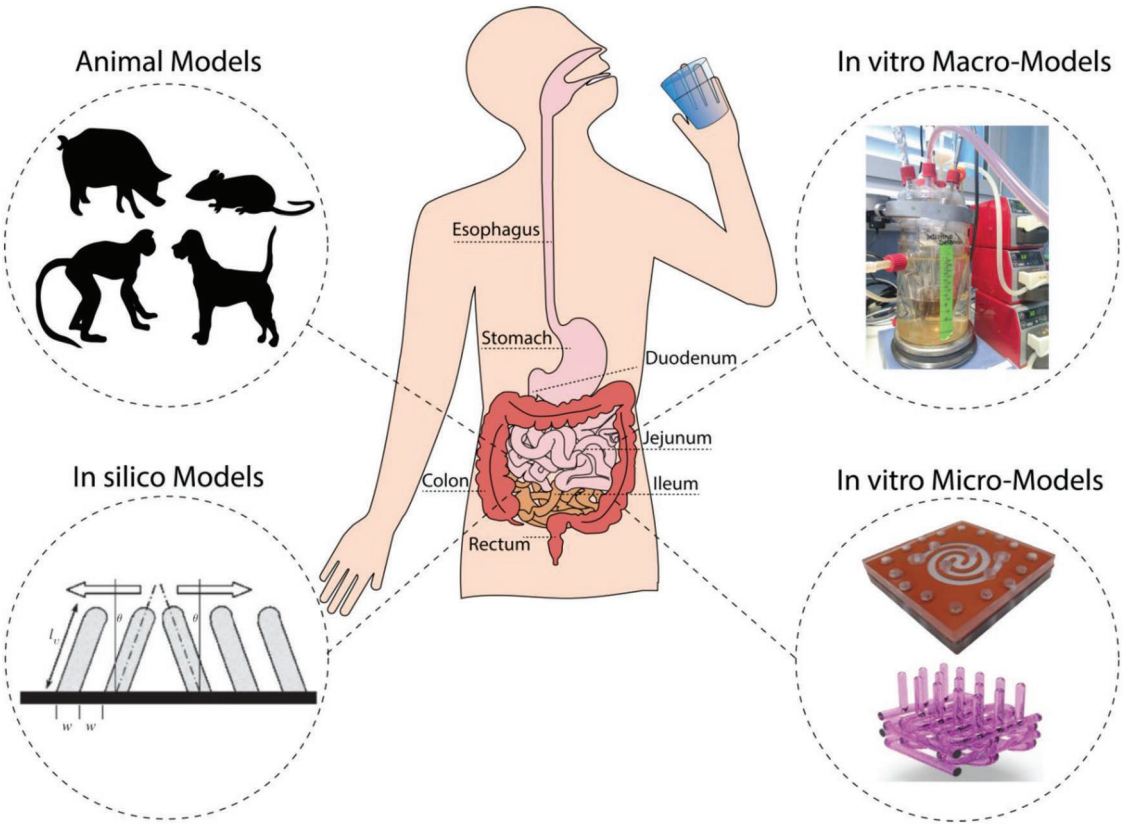

Figure 1. Illustration of the human gastrointestinal tract (GIT) showing the position of the duodenum, jejunum, and ileum, which together form the small intestine, and of the colon, also called the large intestine. Different model categories are represented, which can be used in either food or pharmaceutical studies. The image under in silico models is reproduced with permission.[152a] Copyright 2010, The Royal Society. The macro-models image was provided by Alba Tamargo and colleagues (Institute of Food Science Research (CIAL), Spain).[128b,129] The first in vitro micro-models image is reproduced with permission under the terms of the Creative Commons CC BY licence 4.0.[92] Copyright 2016, the Authors. Published by Springer Nature. The second image is reproduced with permission.[118] Copyright 2018, Elsevier.

smooth muscle layers generate coordinated patterns of contractility termed "peristalsis" and "segmentation."

The epithelial cells are critical for the secretion and absorption of nutrients, electrolytes, and solutes, and the GIT is responsible for the excretion of large amounts of fluid every day. Depending on their location in the GIT, these epithelial cells differ considerably in structure and function. The wall of small intestine is composed by multiple cell types including polarized enterocytes (or intestinal absorptive cells) and other specialized epithelial cells such as enteroendocrine cells (EECs), goblet cells, and Paneth cells.[9] Enterocytes are the main cell type that makes up the intestinal epithelium layer. They are columnar epithelial cells found in small intestine, performing specific digestion of polysaccharides and peptides by the enzymes expressed on their surface. Absorption of nutrients occurs via the microvilli that express on the surface of enterocytes. Microvilli protrude inward into the food contents and increase surface area for the transport of molecules and nutrients from the intestinal lumen into the bloodstream. Enterocyte functions depend on the polarity of the cells. Polarized enterocytes are also essential for establishing and maintaining the integrity of the gut epithelial barrier. Differing from enterocytes, EECs are widely distributed throughout the GIT mucosa. Their functions include secretion of endocrines factors, and regulation of food intake and metabolism.[10] These factors are important for controlling of gut function. In contrast, Paneth cells are responsible for the secretion of growth factors and antimicrobial peptides.[11] The intestinal epithelium consists of ≈4–16% of the goblet cells, scattering among other cells in the epithelium layer. These cells produce mucins, particularly MUC5B and MUC2, that form a mucus layer covering the epithelial cell layer.[12]

Together, the intestinal epithelium represents an essential barrier between the lumen and the intestinal mucosa. In addition to acting as a defensive barrier, the gut contains a host of immune cell types that regulate the immune functions of the GIT. Macrophages, dendritic cells, and regulatory T lymphocytes (Treg) are the major immune cell types found residing underneath the intestinal epithelial monolayer and spread into the mucosa lamina propria. These immune regulatory cells interact with intestinal epithelial cells via factors such as inflammatory cytokines and growth factors.[13] The complexity of the gut immune system has been touched upon in more detail in several recent topical reviews.[14]

2.2. Pathological Conditions of the Gut

Disorders of the gut are complex, and can impede the functions of the intestinal barrier and the mucosa. This can lead to serious

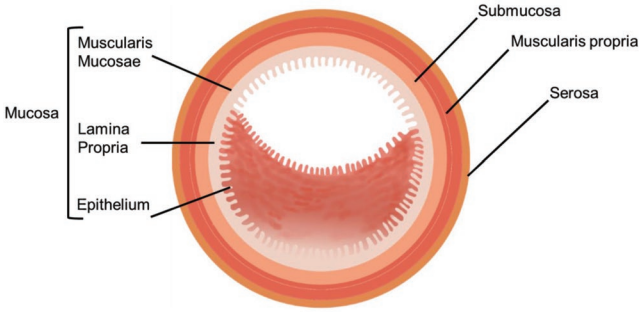

Figure 2. The structure of human intestine. This consists of multiple functional layers including mucosa, submucosa, muscularis propria (longitudinal and circular smooth muscle cell layers), and the outer serosa layers.

diseases of the gut such as IBD, Crohn's disease, ulceration colitis, and gastroesophageal reflux disease (GERD). Even milder forms of these conditions can significantly affect quality of life.

Inflammation represents an underlying pathology common to many conditions affecting the small intestine and has substantial effects on intestinal barrier function. As discussed above, the absorption and transport of nutrients are regulated by the intestinal epithelium. Inflammation is an immunological process that occurs when intestinal tissues are damaged. The bacteria and regulatory immune cells in the intestine are important for immunological functions.[15] Events such as imbalanced bacterial colonization and uncontrolled activation of the immune system can contribute to the onset intestinal inflammatory disease and the development of IBD.

A large number of microorganisms of different species (including bacteria, viruses, fungi, and protozoa) are present in the human GIT, known as gut microbiota. Approximately 1×10^{14} microorganisms exist in the human gut, with most being bacteria.[16] Growing evidence suggests that the gut microbiota and its composition dynamics play a critical role in regulating the physiology and function of the GIT, as well as contribute to gut disorders.[17] For instance, alterations in the gut microbiota populations have been associated with IBD and irritable bowel syndrome (IBS).[18]

2.3. Effects of Diet on Gut Health

Interactions between diet and the colonizing microbiota can impact on gut epithelial integrity and intestinal homeostasis.[17,19] For instance, consumption of diets rich in fats and sugars can change the gut microbiota composition and increase intestinal inflammation,[20] resulting in interruption of the gut permeability and increased levels of proinflammatory cytokines. In the intestine, controlled inflammation is regulated by the regulatory immune cells, particularly macrophages, Treg, and dendritic cells. These cells maintain the intestinal homeostasis by sensing and suppressing uncontrolled immune response from the microbiota-derived or dietary antigens.[21] Changes in microbiota composition can also change the intestinal immune responses by reducing the metabolism of short-chain fatty acids (SCFAs).[22] An imbalance in the microbiota has also been associated with the development of intestinal infections.[23] Thus, it is clear that factors such as diet, microbiota, and the immune system can have an impact on the development of IBD and degree of intestinal inflammation.[24]

Changes in microbiota potentially causative of IBD have also been associated with modifications in food consumption, particularly increased intake of fatty acids, animal proteins, and "fast foods."[14a] In contrast, a Mediterranean diet, including vegetables, fruit, olive oil, cereals, and fish, has been reported to reduce the risk of IBD.[14a] Moreover, malnutrition and deficiencies in micronutrients have been described in patients with IBD[25] and chronic intestinal disorders, respectively.[26] Additional factors such as genetic, environmental, microbiota disequilibrium, and immune dysregulation also contribute to the development of IBD.[27] Although challenging, understanding the roles and mechanisms of intestinal microbiota, food composition, intestinal mucosal immunity, and environmental factors in preserving gut health may provide fundamental insight into the development of future foods for health.

3. In Vivo Animal Models

Animal models have many advantages over doubled-blind randomized clinical trials (RCTs) for assessing the impact of diet and pharmaceutical products for gut conditions. While human clinical trials are highly translational in terms of public health policy changes, there are many challenges regarding their conduct. These include ethical issues, designing and managing studies, high dropout rates, designing appropriate baseline nutritional status, and control groups, as well as effective blinding of investigators and participants.[28] Moreover, factors such as investing the direct effects of foods and insights into mechanisms have been restricted in human studies.

In this regards, animal models have been developed to study the impacts of food, active compounds, and drugs on their digestion, absorption as well as acute and chronic intestinal inflammation diseases. **Table 1** outlines these model systems and summarizes their relative advantages and limitations.

Rodent (mouse and rat) models have been used extensively to study intestinal injury and disease.[29] Chemicals such as dextran sodium sulfate (DSS) and trinitrobenzene sulfonic acid (TNBS) used to incite acute inflammation are used in both mouse and rat models.[30] Rodent models can also be genetically modified to study the role of individual genes on gastrointestinal conditions.

Immunologically compromised mouse models have been extensively employed to study the immune responses during intestinal damaged or infection. Models can feature genetic deletion of immune factors or changes that activate proteins involved in pathogen recognition necessary to trigger both innate and adaptive immune responses. Common knockout genes used in mouse models associated with adaptive immune responses are interleukin 10 (IL-10), interleukin-23 receptor (IL-23 R), cluster of differentiation 4 ($CD4^+$), cluster of differentiation 25 ($CD25^+$), transforming growth factor beta 1 (TGF-β1), recombinant activating genes (RAGs), interleukin 2 (IL-2), signal transducer and activator of transcription 3 (STAT3), nuclear factor kappa-light-chain-enhancer of activated B cells (NFκB);[31] innate immune responses are nucleotide-binding oligomerization domain-containing protein 2 (NOD2/CARD15),

Table 1. Summary of common animal models for intestinal studies.

Species	Body size	Intestinal length and weight	Application in research	Advantages and limitations	Ref.
Mouse	40–45 g	33–40 cm 1.2 g	Inflammatory and immune responses Inflammatory bowel disease (IBD) studies Gut microbiomes and diet studies	Relatively low cost and easy to maintain Rapid production rate Easy to create transgenic models Small sample size Differences in pathophysiological and clinical signs of diseases Technically difficult for surgical techniques due to the small size Genome: ≈14% smaller than humans	[32,42]
Rat	140–500 g	105–115 cm 6–7 g	Inflammatory and immune responses Nutritional studies Drug absorption and metabolism Microbiome studies	Relatively low cost and easy to maintain Rapid production rate More tissue samples can be harvested as compared to mouse Differences in pathophysiological and clinical signs of diseases	[33,43]
Pig	200–300 kg	15–22 m 2310 g	Bioavailability and absorption of nutrient Intestinal transporters and enzymes Gut microbiota and inflammatory responses Microbiota studies	Comparable microbiome Genome: ≈7% smaller than humans Exhibit pathophysiological and clinical signs of diseases High cost and maintenance Difficult to manage and handling	[37b,44]
Dog	10–15 kg	283 cm 263 g	Gut microbes and gut–brain–axis studies Drug absorption and metabolism	High cost and maintenance Comparable microbiome gene content and in response to diet Difficult to manage and handling	[38,45]
Nonhuman primate	5–8 kg	40–64 g	Gut microbiomes and diet studies Drug absorption and metabolism	Genetic close to human Responses of microbes to diet different compared to human High cost and maintenance Ethical challenges	[40,46]

adenomatous polyposis coli ($APC^{min/+}$), toll-like receptor (TLR);[31b,c] both adaptive and innate immune responses are autophagy related 16 like 1 (ATG16L1), tumor necrosis factor alpha (TNF-α), mucin 2 (MUC2), Interferon gamma (IFN-γ), myeloid differentiation primary response 88 (MyD88).[29a,31a,b] Mice are viewed as favorable models due to their relatively similar intestinal development, immune responses, and genetic elements compared to humans.[32]

In comparison, rats have the advantage of being larger; hence, more substantive tissue samples can be harvested. Rat models are often used in nutritional studies such as the influence of fiber-rich diets on intestinal microbial community.[33] Rats can also be genetically modified to model gut disease. For instance, HLA-B27 rat strain colitis has been broadly used for modeling of gut diseases associated with inflammation.[34] Biological incitant *Campylobacter jejuni* has also been used to establish rat model of acute inflammation.[35]

Large animal models (e.g., pig, dog, and nonhuman primate (NHP)) have also been used to investigate intestinal inflammation diseases, microbial communities, and diets. In comparison to small animal models, the GIT of large animals exhibits many features (such as genome, microbiome, and anatomy) that are comparable to the human GIT. This facilitates the investigation of the diet, microbial communities, and intestinal health. Pigs are prodigious eaters and have been employed to study inflammation, immune responses microbiomes, nutrition, as well as the mechanisms involved in the acute and chronic intestinal injury.[36] Anatomically, the porcine intestine and stomach are similar to those of the human.[37] Microbial fermentation, nutrient, and water absorption in the porcine intestine are also comparable to the human intestine.[36c,37b]

Recent studies have shown that the dogs have microbiome gene content and in response to a diet comparable to human microbiome than other species such as mice and pigs.[38] Canine models have been used to identify biomarkers of IBD as they develop IBD and exhibit similar dysfunctional genes to patients with Crohn's disease.[39] NHPs have a high degree of genetic similarity to the human intestine, representing the most comparable model to human. Despite the similarities mentioned above, the gut microbiomes from nonhuman primates have been shown to differ from human microbiomes in response to western diets.[40] Nevertheless, large animal studies are associated with high costs, maintenance, and ethical challenges.[41]

4. In Vitro Cell Culture Models

Numerous standardized in vitro cells models have been developed for the preliminary investigations of toxicity, permeability, absorption, and effect of food and drugs. Ideally, such studies can provide data that guide subsequent animal and clinical trials. The human small intestine is characterized by a remarkable morphological complexity starting with the typical finger-like structure of the villi, which maximizes the surface available

Table 2. Cell lines most commonly used to represent the intestinal epithelium and their characteristics.

Cell line	Origin	Prevalent mucin	Brush border microvilli	Days to polarization
CACO-2	Human colon	Muc5AC[48] Muc3[49]	✓	14–21
HT29	Human colon	Muc5AC[48]	✓	30
HT29-MTX	Human colon	Muc5AC[48]	Shorter than Caco-2[50]	>21
LS174T	Human colon	Muc2[48,49] Muc3[51]	Fewer if compared with Caco-2[48]	–
IPEC-J2	Porcine small intestine	Muc1, Muc3[52]	✓	7–14
MDCK	Canine Kidney	Muc1[53]	✓	–

for nutrient absorption. At the apical position of such structures, the intestinal enterocytes are enveloped with additional microvilli, organized in the so-called brush borders. Furthermore, the lumen is organized with different layers of mucosa and a suite of cellular elements including goblet cells, Paneth cells, stem cells, and Peyer's patches.[47] It is thus difficult to imagine an in vitro model able to perfectly recapitulate such a complex organization of layers, cells and tissues.

The majority of cell models are more simplistic monoculture systems and are based on epithelial intestinal cell lines. These can differ in terms of their molecular and cellular features, as illustrated in **Table 2**.

The most commonly used cell line is the cancer coli-2, or simply known as Caco-2. This cell line was first derived by Fogh et al. in the late 1970s from a 72 years old Caucasian male with colorectal carcinoma.[54] Caco-2 cells naturally differentiate into monolayers of cells with similar properties to those of the human enterocytes, with tight junctions and the typical finger-like structure of the villi. This makes this cell line suitable for representing the intestinal epithelium in vitro.[55] Differentiation takes place in usually 14–21 days, after a confluent monolayer is formed. Despite the long time needed in culturing and maintaining this cell line, Caco-2 cells are still used in food science and medical studies as the absorption properties of these cells correlate well with in vivo data.[55,56] Caco-2 can be cultured and grown on permeable membranes (i.e., Transwell) enabling migration and signaling by secreted factors to be assessed. These cells can also be used in toxicity studies,[57] and to study the effects of food and microbiota.[58] Notably, there are various clones of this cell line commercially available. Among these, the Caco-2 clones C2BBE were later established by Peterson and Mooseker,[59] and improved the in vitro organization of the brush border. Hence, this model is more homogeneous, with villin protein localized consistently in an apical position in contrast to the heterogeneous parental cell line.

HT29 cells are derived from an adenocarcinoma of a 44 years old Caucasian female, and often used to model the human intestine. As with the Caco-2 line, HT29 cells show enterocyte-like behavior and morphology, but require inducers or specific culture conditions to induce this differentiation, which can take up to a month. An advantage of using this cell line is that the cells can spontaneously produce mucin, a key component in the in vivo conditions.[60] The differentiation to mucin-secreting cells is induced with methotrexate and referred to as HT29-MTX. This cell line expresses a high concentration of Mucin-2.

Caco-2 and HT29-MTX cells are often co-cultured to take advantage of the features of both cell lines.[61] The co-culture ratio often used is 90% of Caco-2 and 10% of HT29-MTX, but other studies have been conducted at other physiological ratios, such as 75% of Caco-2 and 25% of HT29-MTX.[61] Other studies have explored the potential of employing additional cell lines, such as Raji B.[62] The goal of such endeavors is to optimize the mucin layer, which has a significant effect even in promoting bacterial adhesion to the epithelium in vitro.[63] Whether co-culturing methods will be superior to using crude mucin is debatable,[63b] and may depend on the bacterial strain being tested.

LS174T is an alternate adenocarcinoma-derived cell line, and has also been used to model the human intestine. One of the main differences between intestinal cancer-derived cell lines is the production of different types of mucins at different concentrations. The goblet-like LS174T cells are reported to express higher amounts of MUC2 if compared with other epithelial cells.[48,49]

The IPEC-J2 is a nonhuman cell line derived from the small porcine intestine.[64] The IPEC-J2 enterocytes spontaneously polarize in around 14 days, and the cell line is often preferred for its noncarcinogenic origin and it shows high values of transepithelial electrical resistance (TEER), even higher than the TEER measured in vivo.[65]

Finally, the Madin–Darby canine kidney (MDCK) cells are a nonintestinal cell line derived from kidney tubules, and used to study cell permeability and infection.[66] MDCK cells can polarize into a confluent monolayer forming tight junctions, and differentiate rapidly (between 3 and 6 days).[67] However, the relevance of this line has been called into question by a study showing that the basolateral transport of the MDCK cell line is different from that of Caco-2 cells, and more importantly, the permeability values found in this study do not adequately represent absorption in humans.[68]

The use of intestinal stem cells has been more recently explored in the development of intestinal organoids and cell structures which are able to recapitulate their 3D organization naturally occurring in vivo.[69] However, when culturing organoids, the use of an extracellular matrix (e.g., Matrigel or collagen) is fundamental for their adhesion and growth. Because of the variation in composition of the different matrices, which are also animal derived, more research has been done in this area for the development of new matrices which might be later standardized for specific applications. Lutolf and co-workers[70] have designed ad hoc matrices for intestinal stem cells and organoids culture, showing that the stiffness of the matrix has a relevant impact on cell signaling and growth. Furthermore, their matrix was validated for mouse-derived intestinal crypts as well as human small intestine- and colorectal cancer-derived cells, highlighting the adaptability of their application.

5. Microfluidic In Vitro Systems: the IsOC

Over the last decade, microfluidic systems, known as organs on chips, have emerged as cost-effective high-throughput systems for in vitro modeling of the GIT. The body-on-chip concept can be traced back to early 2000, when cell culture analogous microdevices gained more consideration as alternative testing tools.[71] With microfluidics, cells are cultured in engineered micrometer-sized chambers, constantly perfused with the required nutrients. The capacity to introduce constant fluid flow and to operate with lower cell numbers makes them superior to many static in vitro systems. The presence of continuous fluid flow has been proven to be beneficial to cell lines cultured in microfluidic IsOC devices. Cells cultured under these conditions polarize faster than on static multiwell plates and express higher amounts of specific proteins such as mucin. The use of continuous flow can mimic dynamic actions of bodily fluids in terms of mechanism and forces (e.g., blood flow, peristalsis, and shear stress). Additionally, customizability of microfluidic devices allows for more specific representations of cross-talk between various defined cell lineages. The addition of chambers and channels of different sizes enables a more meaningful downscaling of the phenomena of interest, taking into consideration features such as proportions between different organs or the ratio between different types of cells. In contrast, the studies on standardized multiwell plates are limited to the space made available in the commercialized devices. Microfluidic systems hold significant potential for drug development and high-throughput screening. Currently, producing and validating a novel pharmaceutical has been reported to average 10–15 years and 2.6B dollars.[72] A component of these costs is drug failures due to safety and efficacy issues, which can be expensive at latter stages of development.[73] Microfluidics enables testing in human cells to identify safety and efficacy issues undetectable by preclinical animal models. Indeed, animal models are not flawless; BIA 10–2474, the fatty acid amide hydrolase inhibitor, led to fatalities and severe adverse events in a clinical trial, despite earlier animal tests.[74]

Microfluidic devices are fabricated with standard soft lithography techniques that enable high precision. Briefly, a silicon wafer is used as a substrate, and it is coated with photoresist for the later exposure and the final development of the desired design. Polydimethylsiloxane (PDMS), or more recently alternative compounds,[75] is cast onto the fabricated silicon mold. Designs can be produced as small as a few micrometers and tailored to different cell systems. Once a system is established, conditions such as cellular shear stress can be modulated by altering the flow rates of the media continuously perfusing these chambers. This has particular relevance to modeling the human intestine, where peristaltic motility and fluidic shear play an important role on the epithelium and this organ's transport and absorption dynamics.

A seminal 2008 study published by Kimura et al. described a multichannel microfluidic system (**Figure 3**A–D) for intestinal tissue modeling, i.e., an Intestine-on-chip (IOC).[76] They reported the use of Caco-2 cells, and in the case of intestinal cell cultures, the modulation of the flow rate could promote cellular polarization in a time more rapid than static multiwell plates.

5.1. Food and Drugs Studies

Sophisticated models are required to study absorption, distribution, metabolism, and excretion (ADME) of active compounds or drugs in the human digestion system. Organs-on-chips facilitate study of each ADME step individually and offer detailed characterization of compound behavior. Microfluidic devices for PK and PD models have also been developed.[71a,77] Mathematical models have been generated for PK and PD prediction. For instance, modeling of the anticancer drug 5-fluorouracil yielded toxicity dynamics subsequently validated through microfluidics.[77b] PK–PD studies are important for high-throughput drug screening, as illustrated by tests for the anticancer activity of lutein.[78]

The Caco-2 model of IsOC has been extensively used to assess the permeability of the cellular monolayer.[75,79] This allows insight into how drugs may disrupt the tight junctions of the cell monolayer. IsOC and organs-on-chips are able to appraise the toxicity and drug efficacy rapidly, and can also examine transport using Transwell style inserts. The lower consumption of reagents and more conservative use of cells can reduce culture requirements by up to 80% compared to commercial inserts.[80] For food-related studies, a platform called "NutriChip" (Figure 3E–G) has been used to measure the immunomodulatory properties of dairy products.[81] Compared to other IsOC models, they incorporate fluorescent outputs enabling the in situ detection of cytokines released by macrophages. This system also had utility in measuring calcium transport through the epithelial layer, using Caco-2 cells.[82] Other studies have used microfluidic IsOC systems to analyze transport of lipophilic dioxin,[79a] the flavonoid apigenin,[83] and soy isoflavone.[84] Finally, IsOC systems have been shown to mimic gut injuries from viral infections[85] or from γ-radiation,[86] with Caco-2 cells losing their villi morphology and barrier function. Co-cultures with other cells such as the mucus-producing HT29-MTX,[87] or the U937 for inflammation-related studies,[88] and the use of human-derived organoids[86,89] have further improved these IsOC platforms. In the case of the mucus-producing HT29-MTX, these goblet-like cells are used to mimic the mucus layer naturally present in our gut. The inclusion of a mucus layer in in vitro models is highly relevant in permeability and barrier integrity studies as the model results better reflect in vivo conditions. The use of gut organoids has also been implemented in IsOC. Derived from biopsy samples or pluripotent stem cells, organoids are seen as a more meaningful representation in terms of genetic background if compared with the carcinoma-derived cell lines. In fact, they can be derived from healthy subjects as well as from individuals affected by the most diverse conditions, allowing the studies in vitro to be patient specific.[90] Furthermore, it has been shown how confluent monolayers of gut organoids can be cultured for up to 2 weeks[89] and polarized inside IsOC under microfluidic flow.

5.2. IsOC for Host–Microbiota Co-Cultures

In vitro modeling of the gut microbiota can prove challenging. The human intestine has a rich diversity of microorganisms,

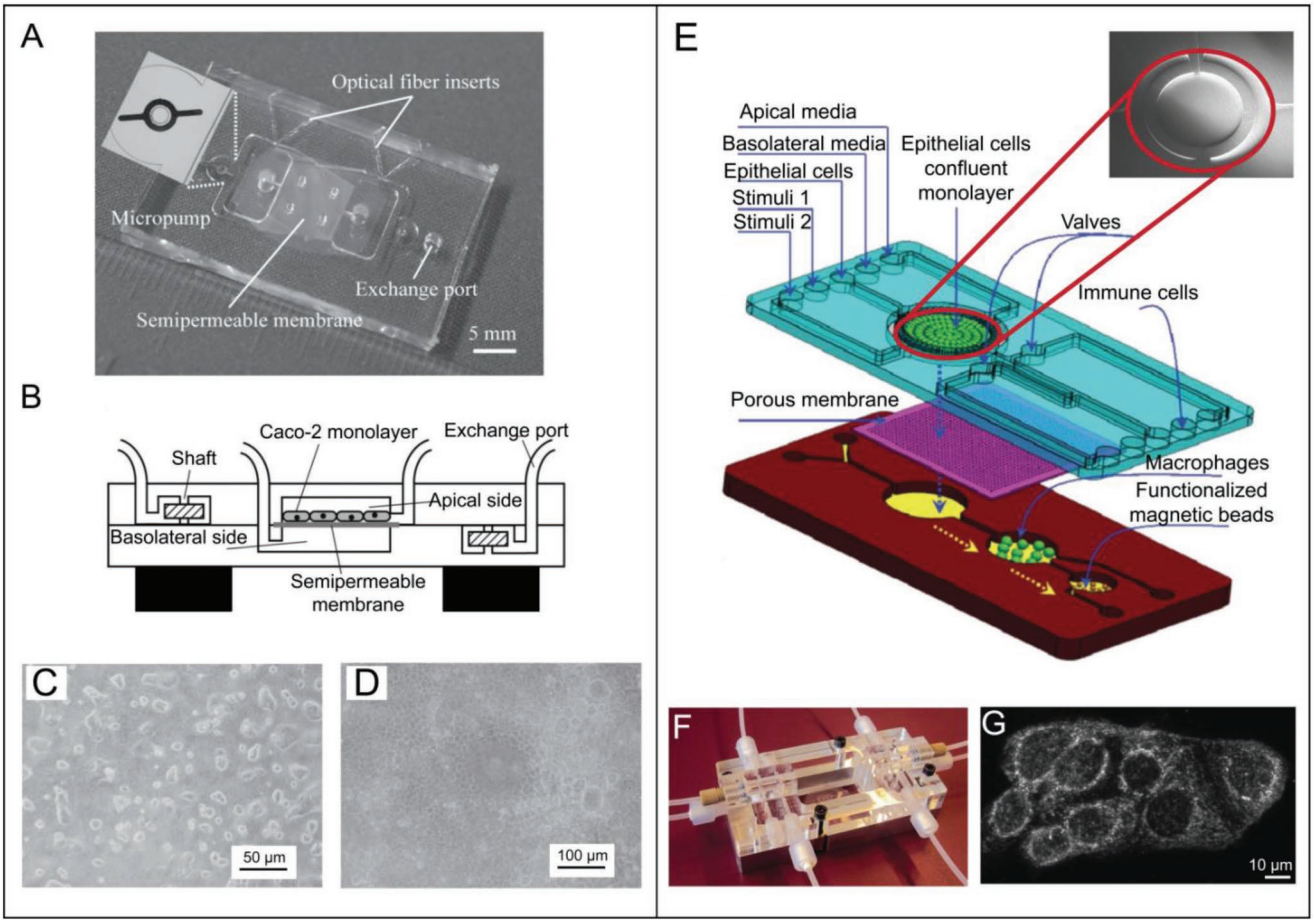

Figure 3. Microfluidic Intestines-on-chips (IsOC). A) Photo of one of the first IsOC platforms by Kimura[76] featuring an on-chip micropump and the integration of optical microfibers for the quantification of fluorescent molecules on-chip. B) Schematic of the chip showing the two chambers separated by a semipermeable membrane on top of which epithelial cells are cultured. (C) and (D) show Caco-2 cells at day 1 and at day 21 post-seeding respectively, highlighting that the cell monolayer can be cultured for prolonged duration. (A–D) Adapted with permission.[76] Copyright 2008, The Royal Society of Chemistry. E) Illustration of the "NutriChip"[81a] setup showing the apical and basolateral chambers separated by a porous membrane. In red is shown a zoom of the micro-fabricated perfusion channels featured in the apical chamber; F) Photograph of the same IOC setup for the study of immuno-modulatory effects of dairy products. G) A fluorescent picture of Toll-like Receptor 2 expressed in Caco-2 cells after induction of inflammation with lipopolysaccharide (LPS). (E–G) Adapted with permission.[81a] Copyright 2013, The Royal Society of Chemistry.

with microbes contributing to digestion in both small and large intestines. Static in vitro multiwell plate systems are limited in their capacity to incorporate microorganisms, and animal models can differ in terms of gut microbiota and the functionality of this flora.[4a] IsOC systems, in contrast, can be used to model interactions between microbiota and human intestinal cells.

Lactobacillus rhamnosus (LGG), isolated from the human intestine, was successfully co-cultured with Caco-2 cells inside an intestine-on-a-chip device.[91] Co-culture was shown to improve the barrier function of the intestinal cells. Wilmes and co-workers improved upon this work with their human–microbe device, "HuMix."[92] Again, *L. rhamnosus* was co-cultured with Caco-2 cells, this time in anaerobic conditions more analogous to the human intestine. The obligate *Bacteroides caccae* was also cultured in one of the chambers of the "HuMix" (**Figure 4**A–D). Transcriptomic and immunological analyses based on the culture of Caco-2 cells with either solely *Lactobacillus* or *Lactobacillus* and *B. caccae* together showed different responses and genes expression in Caco-2, comparable to other in vivo studies in humans and piglets.[92] Hence, this study underscores the importance of host–bacterial cross-talk on host–cell function.

A subsequent study on co-cultured Caco-2 cells with VSL#3 formula containing eight strains of lyophilized probiotic bacteria (*Lactobacillus bulcaricus, Lactobacillus acidophilus, Lactobacillus paracasei*, and *Lactobacillus plantarum; Bifidobacterium infantis, Bifidobacterium longum,* and *Bifidobacterium breve;* and the *Streptococcus thermophiles*).[93] Integrating the microbiota on-chip showed how the probiotics increased the host cellular differentiation and were beneficial when modeling infection by introducing the pathogen *Escherichia coli*. The enterovirus *coxsackievirus B1* was also used to replicate an infection-on-chip showing that Caco-2 cells lost their finger-like morphology and protective functionality.[85] More recently, the same IOC device was used for recreating a more complex environment including aerobic and anaerobic microbiota co-cultured with Caco-2 and intestinal microvascular endothelial cells.[94] *Bacteroides fragilis*, an obligate anaerobe bacterium,

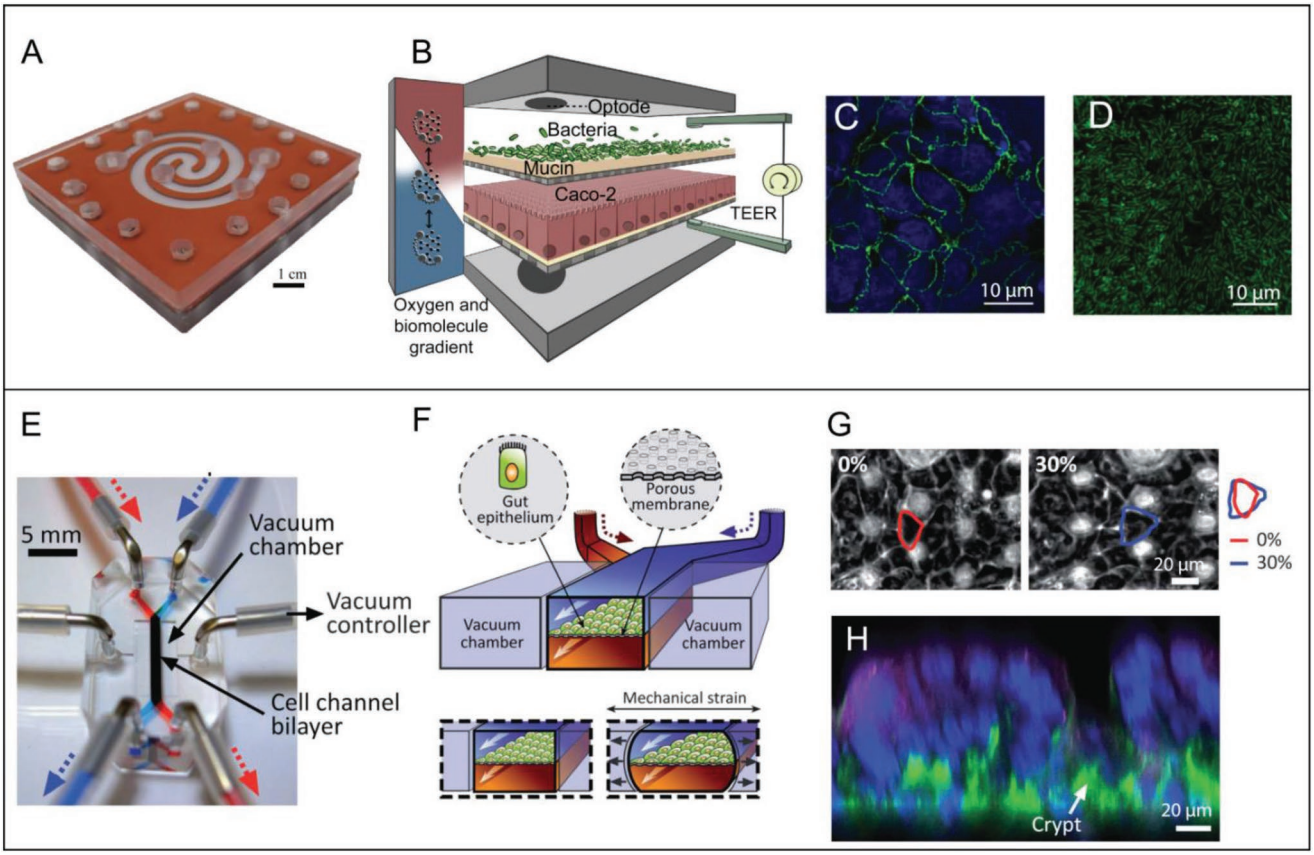

Figure 4. Microfluidic Intestines-on-chips (IsOC). A) The "HuMix"[92] for the study of Human Microbial Crosstalk. Photo of the device and (B) schematic representation of the setup with two membranes used for epithelial Caco-2 cells and bacteria; (C) immunofluorescence image of Caco-2 cells co-cultured for 24 h with *Lactobacillus rhamnosus* (LGG) (nuclei stained in blue, and occludin in green); (D) live-dead staining of LGG post-24 hours co-culture showing in green the viable LGG. (A–D) Adapted with permission under the terms of the Creative Commons CC BY licence 4.0.[92] Copyright 2016, the Authors. Published by Springer Nature. E) The "Gut Chip"[91] platform by Ingber and others (Emulate Inc.) showing the two vacuum chambers used to apply cyclic strain to the epithelial cells; (F) schematic of the chip functioning and (G) phase contrast images of Caco-2 cells showing variation in their morphology before and after applying cyclic strain; (H) confocal image of the cells showing the typical intestinal villi morphology; the cells were stained after around 7 days in the microfluidic chip for nuclei (blue), F-actin (green), Mucin-2 (red). (E–H) Adapted with permission.[91] Copyright 2012, The Royal Society of Chemistry.

was grown in the chip for more than 3 days in co-culture with the cells. The anaerobic conditions were recreated in this chip, and oxygen concentration levels were monitored via sensor integration. The co-culture was also possible thanks to the cells developing a mucin layer; this was fundamental for bacteria adhesion and it is possibly one of the reasons why cell-microbiota cultures can be performed on-chip for longer times. Testing of different microbiota compositions from human fece samples was also performed on this chip, and it was confirmed that *Bacteroidetes* and *Firmicutes*, as well as other obligate species, were more abundant under anaerobic conditions, proving the importance of a good oxygen control. Furthermore, primary intestinal epithelial cells from biopsies were also cultures in lieu of Caco-2 cells to explore whether more complex cell lines could be used in co-culture with microbiota isolated from adults and infants' fece samples. Aside from a variation in bacteria abundancy being prevalent in the adult samples as predicted, in both cases, microbiota primary cell co-cultures were maintained inside the IOC for at least 5 days under microfluidics conditions.

5.3. Emerging Developments in IsOC

Online monitoring devices can be integrated with sensors for real-time control of microfluidic systems and measurement of cellular parameters. The integration of micropumps within the same device allows for simpler setups, avoiding the use of external pumps (Figure 3A).[76] In the case of the IsOC, it is important to develop a peristalsis-like flow to closely mimic in vivo conditions. Ingber's team has developed a proprietary microfluidic intestine device (Figure 4E–H), named the "Gut Chip" (Emulate, Inc.) that uses lateral vacuum chambers connected to a controller to regulate the suction force.[91,93–95] This further reduced the time to polarization of Caco-2 cells to 5–7 days. More recently, MIMETAS B.V. (The Netherlands) has proposed a unique IOC called "OrganoPlate" (**Figure 5**A–C) that enables culturing of epithelial cells inside a tubular-shaped channel. The OrganoPlate does not require the use of artificial membranes employed in other IsOC or in Transwell inserts. In this device, a rocking system is also used to ensure efficient media exchange within the microfluidic chambers.[96] In terms

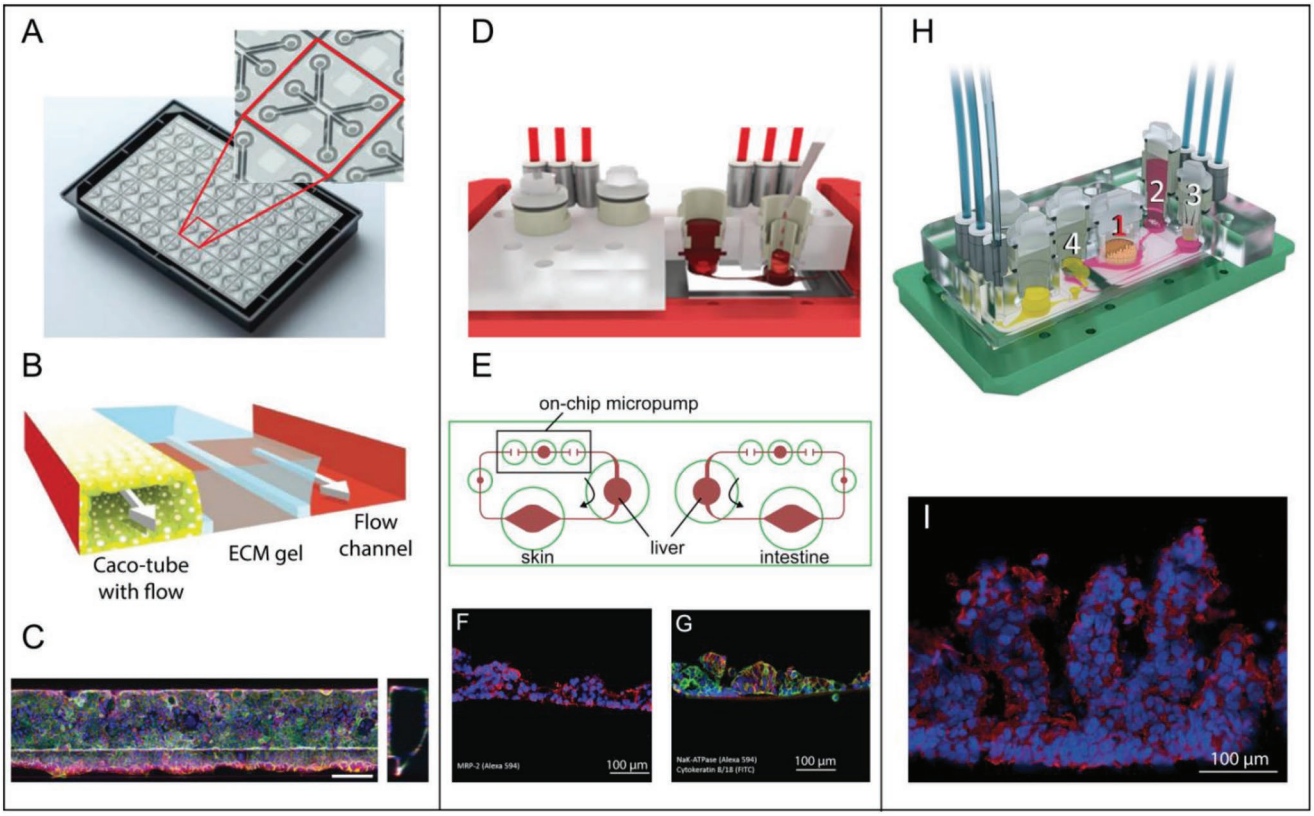

Figure 5. A–C) "OrganoPlate" by MIMETAS B.V.[96] An image of their plate with 40 cell culture microfluidic structures in a 384 well-plate type; schematic of each chip with 3-lanes; immunofluorescence images of Caco-2 cells inside the tubular channel, z-stack and max projection, with staining done for Zonola Occludens ZO-1 (red), and Ezrin (green) (scale bar 100 µm). (A–C) Adapted with permission under the terms of the Creative Commons CC BY licence 4.0.[96] Copyright 2017, the Authors. Published by Springer Nature. D–G) "Multi-Organ Chip" by TissUse GmbH and MatTek Corporation.[99] D) Schematic of the device showing the compartments used for the liver–intestine culture and (E) re-drawn circuits for the co-culture in parallel of the skin–liver and liver–intestine systems which use micropumps on-chip; the arrows indicate the flow direction. F,G) Immunofluorescence images of intestinal tissues showing expression of (F) MRP-2 (red), (G) NaK-ATPase (red) and cytokeratin 8/18 (green). Nuclei staining is shown in blue in both pictures. (D–G) Adapted with permission.[99] Copyright 2015, Elsevier. H,I) The "Four Organs-chip" by TissUse GmbH. (H) shows the set-up with the four organs-chip numbered in order (1) intestine, (2) liver, (3) skin, (4) kidney. (I) shows immunofluorescence staining of the intestinal tissue after 28 days where nuclei are stained in blue and cytokeratin Ctk 19 is shown in red. (H,I) Adapted with permission.[100] Copyright 2015, The Royal Society of Chemistry.

of measurement, IsOC can be integrated with optical fiber systems for gauging pharmacokinetic parameters with real-time online fluorescence,[76,81a] or with sensors for the measuring dissolved oxygen.[76,92,94] In the "Nutrichip," a complementary metal oxide sensor (CMOS), was also used for a real-time measure of fluorescence detection of cytokines.[81] When culturing epithelial cells, measures of the TEER are used to assess the quality of the cellular tight junctions. This can be done under dynamic conditions on-chip by coupling the chip with special versions of electrodes.[91–93] The direction of the flow can influence cellular shear stress and nutrient renewal, with the majority of IsOC using a horizontal directionality of flow. However, a recent publication has described the use of perpendicular flow; centrifugal force was used to seed intestinal cells in a disk-shaped microfluidic chip with the aim of reproducing the tubular-like morphology of the native intestine. This system yielded increased expression of proteins such as villin and mucin.[97]

An exciting advancement is the combination of multiple organ-on-chip systems connected on the microscale. Yoshimura and co-workers have developed a micrototal bioassay with integrated small intestine and liver on-chip for a study of intestinal absorption and liver metabolism of various anticancer substances.[84] The cross-talk between different organs can greatly inform ADME studies. Inflammatory[98] and drug toxicity[99] studies have been developed on gut–liver chips to investigate the cross-talk between liver and gut (Figure 5D–G). The same gut–liver system by Maschmeyer et al. (TissUse GmbH, Germany and MatTek Corporation, USA)[99] uses a skin–liver circuit for parallel studies of drug administration. The shape of the channels (Figure 5E) is designed to reduce specific shear stress values to avoid damaging the tissues samples. In their "MultiOrgan Chip" system, the co-cultures are intended to reproduce in vivo organs at the smallest acceptable scale of 1/100 000. Primary intestinal epithelial cells are obtained from a biopsy of a healthy human small intestine and cultured in this gut-on-a-chip to establish an in vitro model of the intestinal barrier. In a study to experimentally validate the model, intestinal cells showed expression of the transporters multidrug resistance–associated protein 2 (MRP-2),

and sodium–potassium pump NaK-ATPase after 14 days in microfluidic co-culture (Figure 5F,G). A similar chip concept by TissUse GmbH was adopted in an emerging commercial system that enables the co-culture of up to four different organs on chip.[100] Figure 5H shows the setup for the four organs system where intestine, liver, kidney, and skin are numbered in order. The system is able to recapitulate the more complex villi architecture (Figure 5I) over 28 days of microfluidic co-culture.

Despite their numerous benefits, the capacity of IsOC to represent the complex interactions between human organs remains incomplete. Further advancement needs to be made in terms of recapitulating both healthy and diseased tissues. This may be further promoted by materials' development, such as finding substitutes for PDMS.[101] While PDMS is clear, flexible, heat resistant, and enables gas exchange, it can absorb hydrophobic substances and can interact with polar compounds.[102] The latter drawback is critical for PK–PD studies. Alternatively, solutions have been proposed in terms of PDMS functionalization.[103]

The various IsOC models that have been discussed have contrasting advantages and disadvantages such that no individual device is clearly superior to all applications. There is an intrinsic trade-off between complexity and biological relevance such that those devices that most accurately replicate the fluid flow, cell types, and cell–cell interactions can be the most challenging to produce and utilize. As an example, the NutriChip[81] is a powerful "food-testing" platform, but the complexity of the device, involving the use of a complementary sensor for the analysis, might limit its use as a commercialized platform. In contrast, the "HuMix"[92] appears easier to assemble, with larger dimension that would allow for straightforward integration of other sensors (e.g., optode and a TEER probe). The "Gut Chip"[91] is perhaps the most broadly applicable device that is highly adaptable to multiple study designs, but its small dimensions and use of a vacuum controller may be challenging for those unfamiliar with microfluidics. This can be juxtaposed with the "Organo-Plate" by MIMETAS[96] or the "Multi-Organ Chip" by TissUse GmbH,[99,100] which adopt more of a "plug and play" approach that may facilitate their use as a standardized platform.

As IsOC are still in a phase of innovation and elaboration, there are no standardized systems that are used across laboratories. This can make it challenging for microfluidic IsOC and organs-on-chips to be accepted as robust research tools. However, this acceptance is likely forthcoming as companies with patented IsOC platforms seek to establish these systems (e.g., MIMETAS B.V., The Netherlands; Insphero, Switzerland; Emulate Inc., USA; TissUse GmbH, Germany; and CN Bio Innovations Ltd., UK). In 2017, the Food and Drug Administration (FDA) signed agreements with both Emulate, Inc. and CN Bio Innovation allowing their IsOC and organs-on-chips platforms for toxicity studies. In 2018, Roche signed a cooperative agreement for using TissUse's platforms in vitro assays as did AstraZeneca and Emulate Inc. NASA has, in collaboration with NIH (NCATS), commenced studying the effects of microgravity through these multiorgan systems.

6. Bioengineered 3D Models of the Small Intestine

Bioengineering of complex 3D systems allows for superior modeling of the anatomical and physiological conditions associated with the gut. In the simplest instance, organoids derived from intestinal epithelial stem cells address some of the main shortcomings of the 2D monolayer and the microfluidic models. The inward epithelial orientation renders their apical surface inaccessible, which is a limitation when modeling native intestinal tissues. The geometrical patterning of the epithelial lining in epithelial organoids greatly differs from that physiological intestines; in that, the villus structures are lacking.[104] To imitate the geometry of intestinal villi and crypts, nonbiological materials can be constructed into villous-like projections on which epithelial cells will be seeded.

Chen et al. described an approach where fabricated hollow lumen structures are made of silk proteins with an internal spiral pattern.[5] Myofibroblasts are dispersed into the porous silk scaffold on which Caco-2 and HT29-MTX epithelial cells were seeded. The 3D architecture of this model resulted in favorable orientation of epithelium monolayers, established an oxygen gradient, and generated both aerophilic and anaerobic microenvironments. More realistic geometries could be developed by combining multiple fabrication techniques. Arrays of sub-millimeter long (≈400–500 μm) villous-like features with a tip diameter of ≈50–100 μm were fabricated following a multistep, multitechnique fabrication procedure. The negative mold was first developed using laser ablation or micromilling on a plastic substrate, followed by casting the PDMS-based mold. The PDMS mold was then used as the negative mold for the second scarifying mold that can be easily dissolved (e.g., ionically cross-linked alginate and agarose).[105] This scarifying mold was then used for casting the final 3D construct which can be made of hydrogels such as collagen, gelatin, hyaluronic acid, poly(ethylene glycol diacrylate) (PEGDA), or thermoplastics such as poly(lactic-*co*-glycolic acid) (PLGA) and poly(ethylene-*co*-vinyl acetate) (PEVAc) (**Figure 6**A).[105,106] To facilitate the transport of nutrients and encourage cell growth, the matrix requires a porous or fibrous microstructure. In the case of hydrogels, pores are introduced via lyophilization. For thermoplastic-based scaffolds, the porous structure can be developed by incorporating scarifying particles into the material prior to the final stage of molding followed by their removal with a solvent. These 3D scaffolds are then used for co-culturing of epithelial cell types and select bacteria populations such as *Salmonella*, *Pseudomonas*, *Lactobacillus*, and *E. coli*.[106c]

The complex topography of intestine can also be fabricated by 3D bioprinting,[107] which considerably reduces the number of processing steps and enables upscaling of the model. In this approach, printable inks based on soft hydrogels are extruded through a nozzle following the computer-aided design (CAD) of the intended construct. Various synthetic and natural hydrogel systems have been used for gel printing.[108] These include PEG dimethacrylate (PEGDMA),[109] gelatin methacrylate (GelMA),[110] Lutrol,[111] gelatin,[112] gelatin/chitosan,[113] fibrinogen/collagen,[114] alginate/gelatin,[115] alginate/gelatin/fibrinogen,[116] and combinations of synthetic and natural hydrogels.[117] Kim et al. used Caco-2 cell-laden collagen as the bioink mixed with tannic acid for cross-linking immediately before gel printing of 500–1000 μm long villous features with a base diameter of ≈200 μm (Figure 6B).[118] The initial cell viability after printing and cross-linking was over 90%. Interestingly, the model fabricated by cell-laden bioinks exhibited

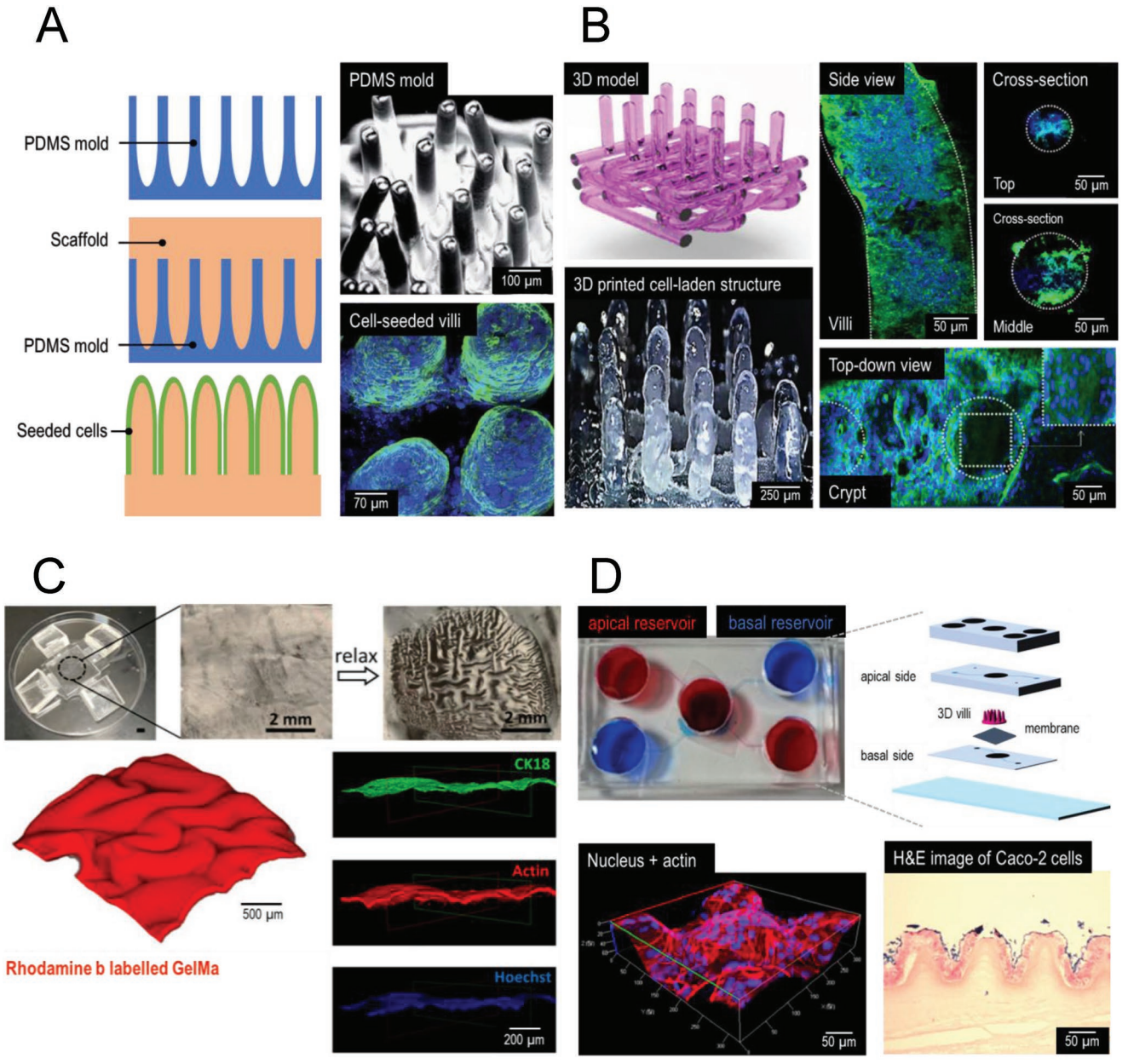

Figure 6. The villi and crypt topography of intestine can be modeled by combining various fabrication techniques. A) Positive PDMS molds made by casting PDMS on patterns plastic, followed by multiple steps of casting to develop the hydrogel or thermoplastic scaffold on which cells are seeded. Adapted with permission.[105a] Copyright 2011, The Royal Society of Chemistry. B) Cell-laden bioinks are 3D-printed to recreate the microstructure of the intestine. Adapted with permission.[118] Copyright 2018, Elsevier. C) Cell-seeded hydrogels are cast on top of bilaterally deformed tough hydrogels, where upon the release of stress the cell-seeded layer wrinkles and generates a villi–crypt topography. Adapted with permission.[119] Copyright 2018, PNAS. D) The villi structures developed in panel (A) can be integrated in a microfluidic system to provide access to both apical and basal sides of the scaffold. Adapted with permission.[122] Copyright 2017, Springer Nature.

higher cell viability and growth compared to a similar 3D model on which cells were mixed in the ink and were seeded after the fabrication of the 3D model.

In addition to creating artificial villous features, recapitulating the folded patterns of intestinal mucosa in vitro is essential for better representation of intestine in gastrointestinal research. To create the creased pattern of mucosa, Chan et al. cast a layer of GelMA hydrogel with stromal cell line telomerase reverse transcriptase- (hTERT-) immortalized human endometrial stromal cells on a prestretched tough hydrogel substrate[119] (polyacrylamide/alginate hybrid hydrogel). This step was followed by culturing a layer of human endometrial adenocarcinoma cells on top of the GelMA hydrogel film with cultured cells. Upon the release of the prestretching stress, the elastic tough hydrogel returned to its original dimension forcing the top layer of GelMA and epithelial

cells to wrinkle (Figure 6C). The topography of wrinkles was defined by the stiffness of tough hydrogel substrate and the GelMA layer, as well as the prestretching ratio.[119] In another attempt to replicate the multiscale geometry of small intestine, decellularized porcine small intestine was used as the substrate for chemical vapor deposition of Parylene C, followed by gold–palladium sputter coating to increase rigidity and then casting of PDMS to generate the cell-compatible substrate for Caco-2 cells.[120] The PDMS replica topographically resembled the original intestine with clear macro- to microscale features.

Depending on the 3D geometry of the scaffolds, access to the basal compartment of the model can be restricted, hence reducing the characterization assays to those that only require access to the apical compartment. Various strategies have been undertaken to improve the biological relevance of 3D scaffolds. Yu et al. developed a collagen-based villi scaffold on which Caco-2 cells were seeded and suspend this scaffold in a culture well, exposing both apical and basal sides to the culture media.[121] Accessing both sides, this design allowed for drug permeability and TEER studies revealing that the 3D villous models have very close resemblance to actual small intestine epithelium. To access both apical and basal compartments of the model and subject the cells to fluidic shear, the villous scaffold can be integrated into a microfluidic chip with separate microchannels running over and below the scaffold.[106d,122] Separating the apical and basolateral channels permits a higher flexibility for performing a wider range of biological assays (Figure 6D).

7. In Vitro Macromodels

In vitro gastrointestinal models have been designed to simulate the digestion system. These models consist of a series of compartments that simulate the biochemical digestion and metabolism in the gastrointestinal tract with the small and large intestines at the end of the series. While the other in vitro models focus on permeability and absorption studies through the gut epithelium, the macromodels are designed to study the effects of peristalsis, shear stress, and enzymes on food particles' size and structure. Furthermore, these systems can be used to investigate the effect of food or drug on gut microbiota.

Different experimental setups are designed either in vertical or horizontal positions with various methods to reproduce the peristalsis action. These models allow continuous sampling that enable better understanding of the microbial activities. The various parameters (e.g., temperature, pH, flow rates, and pressure) can be precisely controlled by a computer.

The Simulator of the Human Intestinal Microbial Ecosystem (SHIME) was first developed in 1990s at Ghent University, Belgium, and later registered by the company ProDigest. This model consists of interconnected five jacketed glass reactors, representing, respectively;[123] the stomach, the small intestine, and the ascending, transverse, and descending colons (**Figure 7**A). The residence time and pH of each section simulate gastric tract. It is also possible to incorporate microbiota in this model. The SHIME model was used to test the effect of different diet compositions (arabinogalactan, pectin, xylan, dextrins, and starch at different concentrations) on the gut microbiota and volatile fatty acids produced within the simulator.[123] The SHIME simulator has been adopted in a recent study on the metabolism of different polyphenols and oregano-derived luteolin known to be a ligand of the aryl hydrocarbon receptor (AhR), which plays a role in improving gut barrier functions and the intestinal immune defense. In this study, the authors could determine which, among the selected AhR agonists, provide the higher activation of the receptor, with specific attention to the evolution of the fermentation in the different sections of the SHIME.[124] Importantly, when studying microbiota in vitro, one should distinguish between luminal and mucosal microbiota. In this respect, the M-SHIME simulator was designed.[125,126] By introducing mucin agar-coated microcosms at a distal section of the system, the M-SHIME version, allowed for specific colonization of *Clostridium cluster* IV and XIVa. To consider the host–microbiota cross-talk, SHIME has been more recently integrated with a Host–Microbe Interaction (HMI) Module.[127] This in vitro HMI model resembles the intestines-on-chip models' structure, but it has larger dimensions (10 × 6 cm). It consists of a chamber with a porous membrane separating the gut microbiota (top chamber) and enterocytes Caco-2 cells (bottom chamber). Porcine-derived mucin was chosen for different microbial groups' adhesion (*Bifidobacterium*, *Lactobacillus*, *Faecalibacterium prausnitzii*). The HMI module was proven to be functional in recreating the host–microbiota environment, assessing the viability of the enterocyte cells in contact with the gut microbiota and enabling a co-culture for up to 2 days. Finally, the system was connected to the SHIME from which a *Saccaromyces cerevisiae* fermentation product was then flown to the HMI module. The anti-inflammatory properties of the fermented yeast were tested on Caco-2 cells by assessing a lowering of interleukin (IL)-8. However, it should be noticed that in these systems, host cells, mucus layer, and microbiota are separated, while in the microfluidics IsOC systems, previously described, it is possible to integrate the three.[94]

The Simulator Gastro-Intestinal (SIMGI) is another in vitro model of the upper and the lower gastric tract.[128] An extra feature added by this model, developed in 2015 (Spain, Institute of Food Science Research, CIAL), is the peristaltic movement of the stomach which is represented by two cylindrical jacketed containers made of flexible silicone. The peristalsis, at the stomach level, is reproduced by changing the pressure of water flowed around the jacketed containers, which contain different inlets for the mixing of food samples and gastric juices (Figure 7B). SIMGI requires a period of time (1–2 weeks) for the microbiota to stabilize in the different sections before starting any experimental tests. At first SIMGI[128a] was used to study *Bacteroides* found in the first two sections of the colon, while the descending section showed higher production of short-chain fatty acids and a larger presence of *Ruminoccocus*. The total working volumes used by the system are 250, 300, and 400 mL (from ascending to descending colon). SIMGI has been used for studying the effect of various food ingredients and evaluate their modulation effect on the gut microbiota such as grape pomace extracts.[128b–d] More recently, SIMGI was employed to study the antimicrobial effects of silver nanoparticles, which may function as food additives.[129] In this study, the authors tested multiple types of particles for their effects on the metabolic activity and on gut microbiota, and revealed

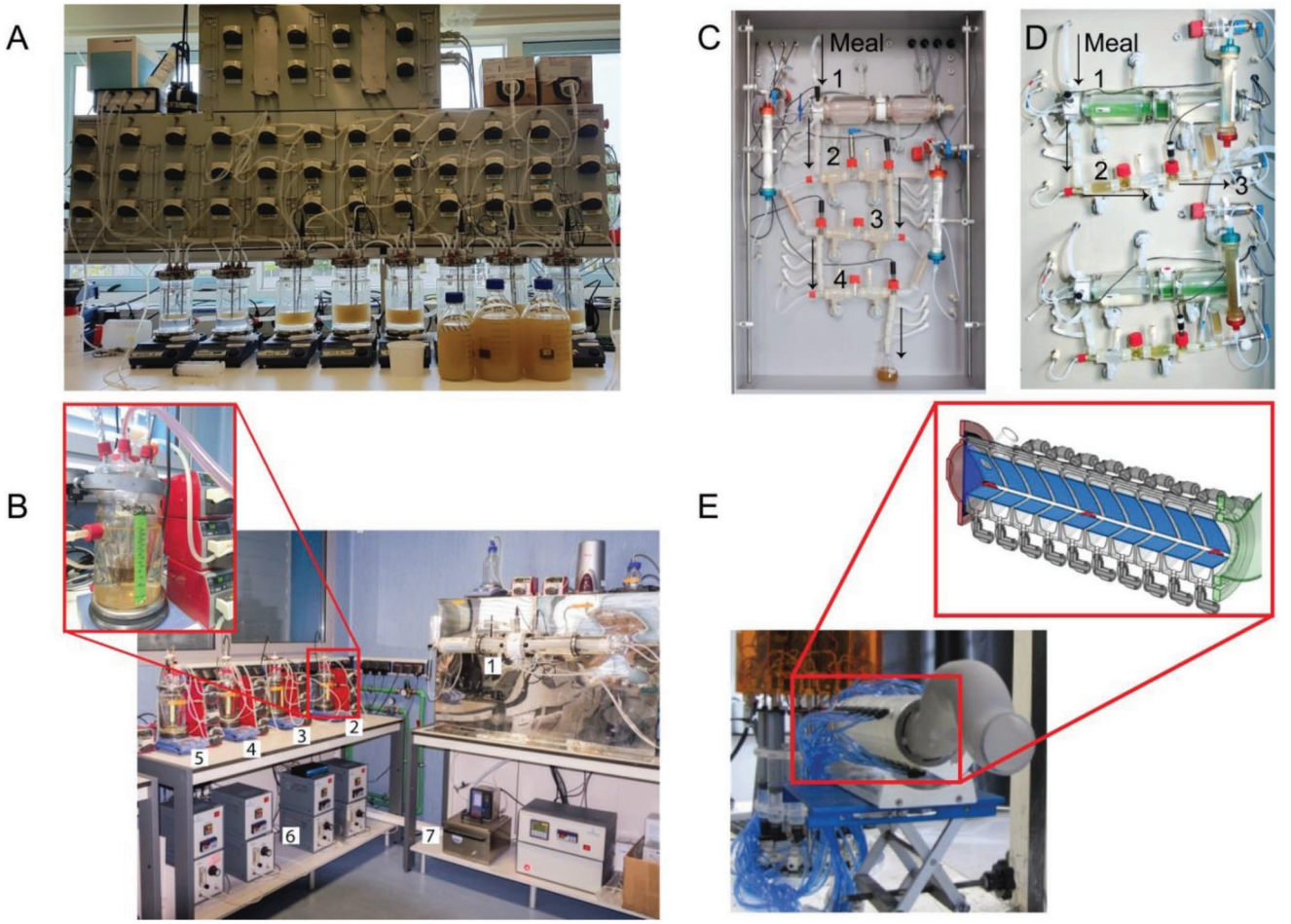

Figure 7. Examples of Macromodels of the human gut. A) A photograph of the SHIME model developed by ProDigest and adopted at Wageningen University.[124] B) The SIMGI gastrointestinal in vitro model.[128b,129] Photo of the entire setup comprising 1) the stomach with peristalsis action; 2) the small intestine; 3) ascending; 4) transverse and 5) descending colon; 6) pH, nitrogen, and temperature controllers, and 7) water bath. The zoom-in panel (B) represents the small intestine compartment. Adapted with permission.[129] Copyright 2019, Elsevier. The detailed picture of the small intestine compartment (zoom) was kindly provided by Alba Tamargo and colleagues from the Institute of Food Science Research (CIAL), Spain.[128b,129] C,D) Photographs from left to right showing in order the TIM-1 and Tiny-TIM. (C) For TIM-1, numbered in order: 1) the stomach compartment, 2) duodenum, 3) jejunum, 4) ileum, and 5) distal secretions. (D) The Tiny-TIM is a simplification of the first system, where the small intestine is not divided but represented as a whole organ. Numbered in order: 1) the stomach, 2) small intestine, and 3) samples collection. The arrows show the direction of the flow. (C,D) Adapted with permission.[135] Copyright 2016, Elsevier. E) The dynamic colon model (DCM) developed at the University of Birmingham: a picture of the setup and zoom of the colon schematic showing the ten "haustra" and the membrane in blue. Adapted with permission under the terms of the Creative Commons CC BY license 4.0.[144] Copyright 2016, the Authors. Published by the International Association for Pharmaceutical Technology.

that all particles increased *Lactobacillus* numbers. This group also tested the effects of prior in vitro digestion, which is a step often lacking in in vitro modeling.

Another example of multicompartment model is the TNO gastro-intestinal model (TIM) system.[130] This model has been used for studying the food digestion, nutrients, and pharmaceutical bioavailability. The system is divided into different horizontal setups with the TIM-1 (Figure 7C) representing the stomach and three parts of the small intestine (duodenum, jejunum, and ileum) and the TIM-2 simulating the colon section. An in vitro mastication is used upfront to recreate digestion at the mouth level. In the first section that simulates the stomach, it is possible to test the digestion of any types of meal or nutrients. Peristaltic valves connecting the stomach section to the others allow for the chime samples to be moved along the artificial gastrointestinal tract. In the artificial duodenum, pancreatin, electrolytes, and bile are used for the digestion. Two filtration sections are used at the jejunum and ileum to filtrate and remove water soluble compounds and products of the digestion. Lipophilic compounds are also removed by a dedicated filter. At the jejunum and ileum sections, pH is controlled by addition of sodium bicarbonate. TIM-1 has been used to study the bioavailability of iron and phosphorus in cereals,[131] anthocyanins from blueberries,[132] and different fortified milk products.[133] It has also been used to study the anti-inflammatory and antioxidant activities of various digested foods.[134]

The Tiny-TIM (Figure 7D) is a smaller version of the TIM-1 that is designed for high-throughput screening of pharmaceutical

products, without separating the small intestine in its three sections.[135] TIM-2[136] is an extension of the TIM system for representing the large intestine in vitro. An important feature of the system is the peristalsis movement reproduced by a flexible membrane, which allows a more uniform mixing than the one offered by the other stirred systems. A dialysis component is also incorporated in the system for removal of microbial acid products, which would lead to microbiota death. Effectively, the peristalsis and dialysis features are important improvements in the series of colon models. TIM-2 has been used for investigating the effect of different maize-derived fibers on gut microbiota,[137] the prebiotic effect of mango peel,[138] cassava bagasse extracts,[139] and plant sterol effects on obese and lean subjects' microbiota,[140] or to investigate the differences between microbiota derived from healthy volunteers and inflammatory bowel disease–affected patients.[141] Furthermore, samples digested in TIM-2 have been further tested on separate cell culture in vitro models for their effect on the immune system,[142] and in Caco-2 cells[143] proving again that different models in vitro can be used in parallel to provide more meaningful information.

An in vitro model of the colon has also been developed by Stamatopoulos et al.[144] Their dynamic colon model (DCM) (Figure 7E) improves the previous existing models, such as the TIM-2, by taking into consideration the important role played by the colon volumetric content, its motility, and physiology in the ascending colon. These are important factors which must be considered when investigating drug delivery and solubility; however, they should be relevant to the in vivo conditions. The DCM consists of an acrylic tube (20 cm long with a diameter of 5 cm) with ten colon pouches (*haustra*), covered by a flexible membrane. The latter is computer-controlled and can be inflated and deflated accordingly to match the in vivo data of the motility functions. With their in vitro system, Stamatopoulos et al.[144] investigated the release of theophylline, a highly dissoluble drug used in the treatment of respiratory disorders. They have established that differences in pressure due to motility, and physiology changes naturally occurring in the gut, have an influence in drugs dissolution and concentration distribution profiles, which are with no doubt important information for both food and drugs studies.

The recently developed "CoMiniGut" (Copenhagen MiniGut)[145] is an example of how fermentation models can be miniaturized. The system consists of five stirred batch reactors, each of them running single fermentations in parallel (four replicates and a control). The novelty of this system is the small working volume used, 5 mL versus 500 mL of the SHIME[125] model and 120 mL of the TIM-2.[136] In their study, Wiese et al. first demonstrated that their system was able to reproduce the colon fermentation of two well-known prebiotics: lactulose and inulin. Finally, they extended the study to the human milk oligosaccharides. These are known to be more expensive, but with the use of such a small working volume, the experimental testing can be cost efficient, allowing the setup to be suitable for studying other rare and expansive compounds. For the inoculum, fecal samples of healthy adults for lactulose and inulin fermentations, and of healthy babies in the case of human milk oligosaccharides, were chosen. This miniaturized system is able to save precious donors' samples as, for the inoculation, only 250 µg of fecal material was needed overall for the five reactors.

"The Smallest Intestine" (TSI)[146] is an in vitro model of the human intestine where small intestine-specific microbiota was developed based on the "CoMiniGut." The TSI system similarly comprises five reactors that test or replicate different compounds at the same time. Each reactor has a working volume of 12 mL, is connected for pH and T controls, and allows for easy sampling. The digestion and absorption in the small intestine are represented in the TSI by changes in pH values, hence by the addition of pancreatic juice, bile salts, and sodium hydroxide at three different stages of the process representing the duodenum, jejunum, and ileum. Small nutrients, electrolytes, and bile absorptions are possible via a dialysis system connected to the reactors and operating continuously. Seven bacterial strains have been used in the TSI in vitro model (*E. coli*, *Streptococcus salivarius* and *Streptococcus lutein-ensis*, *Flavonifractor plautii*, *Enterococcus faecalis*, *B. fragilis*, and *Veillonella parvula*) which were selected as representative of the existing bacterial symbiosis in the small intestine. Other three probiotics strains (*L. plantarum*, *L. rhamnosus*, and *Lactobacillus casei*) have been tested to prove their survival in the system. To the best of our knowledge, the "CoMiniGut" and the TSI system are, at this time, the only in vitro gut models functioning at the smallest volumes, enabling the screening of more expensive compounds. Furthermore, the TSI system takes into consideration the testing of nonfecal bacterial strains, empowering the representation of the human small intestine in vitro.

Other gastrointestinal macromodels have been developed to study food digestion and breakdown in stomach. In fact, models of the stomach can be integrated with other in vitro models of the gut (small and large intestines) allowing a more detailed representation of the gastrointestinal tract, as done by most of the models we have here reviewed. As an example, the human gastric simulator (HGS)[147] is one of the examples of macromodels which use contraction movements to simulate food digestion. The system was first developed at the University of California, Davis in 2010 and also reproduced at Massey University, the Riddet Institute, New Zealand. It consists of the main tubular latex chamber, in which food samples are digested in vitro. Gastric juice secretions are added to the vessel and rollers around it are set and controlled to move, reproducing the muscular contractions naturally occurring in the stomach. Studies on the particle size distribution and the cooking effects on different types of food can be performed on these systems. To conclude, there are internationally recognized protocols for the use of macromodels and for in vitro digestion of a variety of samples, with the INFOGEST consensus connecting researchers internationally.[148]

8. In Silico Mathematical and Computational Models

Computational fluid dynamics (CFD) is a mathematical modeling tool that utilizes the Navier–Stokes equations to model the flow of viscous substances. While it originated in the aerospace industry, the increasing range and sophistication of models as well as the increased availability of high-performance computing has broadened the application of CFD to other areas, including medical applications. Examples of this include

modeling airflow and aerosols in the throat and lungs,[149] blood flow for cardiovascular applications,[150] and modeling of the stomach and intestine.[151] Modeling approaches like CFD are advantageous in that they can reduce the need for experimental research, which can be costly, complex, and ethically challenging. CFD can complement existing experiments by developing methods to visualize the underlying processes.

CFD has been extensively used to model mixing within the intestine.[151b,e,152] This is important since nutrient absorption depends on the transport of the nutrients to the brush border of the intestine. Mixing occurs at a range of length scales; macromixing due to advection of the fluid occurs at scales comparable to the intestinal diameter, while diffusive mixing occurs at the molecular scale. The Reynolds number is the ratio of inertial to viscous forces. In a tube, high Reynolds numbers (>5000) correspond to turbulent flow; under these circumstances, eddies of varying length scales exist; this leads to efficient mixing. At low Reynolds numbers (<2000), the flow is laminar and mixing is poor. Reported Reynolds numbers for flow in the intestine are <200;[152b,153] the majority of CFD modeling has attempted to determine how the motions of the intestinal wall lead to efficient mixing and hence efficient nutrient absorption. Existing models have primarily focused on modeling macromixing in small animals including rabbits (**Figure 8**A,B),[151b]rats,[151e] and guinea pigs.[151e,153] Generally speaking, it was found that the different motions of the intestinal walls promoted mixing within the intestine, and that the rheology of the intestinal fluid had a significant impact on the macroscale mixing. Wang et al.[152a] devised a model of microscale mixing, and their results indicate that motions of the villi induce microscale flow which interacts with the macroscale flow to promote mixing and nutrient absorption (Figure 8C).

Overall it is clear that not all aspects of flow in the intestine are fully understood and CFD offers a way to quantify the complex flow behavior. For the small intestine, the complex rheology of the intestinal fluid, the transient motions, as well as the deformable nature of the intestinal wall are all challenging to model. Major areas for innovation in modeling intestinal fluid dynamics include i) simultaneously simulating multiple motions of the intestinal wall; ii) performing 3D simulations; iii) including improved models of the intestinal wall which take into account its viscoelastic properties; iv) identifying suitable boundary conditions for the wall; and v) including both macro and micromixing in the same model in order to fully replicate physiological behavior. While various modeling approaches (finite volume, lattice Boltzmann, smoothed particle hydrodynamics, etc.) may potentially improve existing models, there is a need to validate models by experimental studies. A mathematical model of the human colon has also been developed by Alexiadis et al.[154] for the study of different mass transport mechanisms (Figure 8D). The in silico model was used in combination with data from the in vitro DCM model developed by the same group[144] which we have reviewed in the previous section (Figure 7E).

The gut microbial community has also been subjected to in silico modeling. By their nature, such modeling activities capture the system in abstract terms and, as such, can serve to elucidate the broader principles governing system behavior.[155] For instance, Faith et al. demonstrated diet as the dominant factor shaping gut microbial community composition within gnotobiotic mice recolonized with a simple community of ten strains and administered well-defined diets.[156] The abundance of each of strain could be modeled as a linear function of dietary protein, fat, and starch, and sucrose content alone. The model was ignorant of host–microbe and microbe–microbe interactions, yet still captured around 61% of variance in community composition. These factors are thus secondary to diet composition in shaping the community, at least for this simplistic collection of diets and microbes.

Three paradigms have predominated efforts to model gut microbial communities. First, systems of coupled ordinary differential equations (ODEs) have described how populations of microbes, their substrates and metabolites, and host cell populations interact in promoting or reducing one another's population sizes. These models are typically aspatial, rendering them suitable for modeling well-mixed systems. Coyte et al.[157] exemplify how modeling can illuminate the principles governing microbial system ecology. Using both ODE- and agent-based (explored below) models of interacting taxa, they explored the ecological foundations of gut microbiome stability, a quality often associated with health. Systems of highly cooperative microbes, supporting one another's growth, were found to be unstable under perturbation: community compositions did not return postperturbation. The reduced abundance of taxa that mutually supports others has destabilizing cascading effects through the network leading to "mutual downfall." Systems of competing microbes exhibited greater stability. Coyte et al.[157] suggest that the host has evolved microbial competition-promoting processes that favor community stability, despite such communities being metabolically less efficient.

Second, agent (aka. individual)-based modeling (ABM) offers a greater articulation of single cell-level dynamics and interactions. Each individual cell in the ecosystem finds explicit representation and location in a spatially explicit environment, and maintains its own individual state. Potentially complex, multifactorial rules governing cellular state changes as responses to environmental cues, intercellular interactions, or stochastic events are specified. By modeling the gut microbiome in terms of trophic guilds, Holmes et al.[158] demonstrated that host provision of nitrogen, e.g., through mucin and urea, is a key factor in shaping microbiome community composition. Through agent-based modeling, single cell-level microbial growth and death dynamics were linked to their capacity to nutritionally satisfy a target 5.2:1 carbon-to-nitrogen ratio. Modeled microbiome community composition was shaped by the balance between diet- and host-derived substrates containing these two limiting nutrients, and the nutritional state of other microbes competing for them. The gut ecosystem is characterized by numerous concentration and profile gradients, such as water, nutrient (e.g., dietary-derived vs mucosal-derived), oxygen, and immune factors (e.g., immunoglobulin A (IgA)), and ABMs are well suited to research questions where these are pertinent.

Lastly, genome scale modeling (GSM) represents microbes at the highly detailed level of their metabolism. GSM construction commences with functional annotation of an organism's genome.[159] Though automated approaches to aid GSM construction are emerging,[160] considerable manual curation remains a necessity.[161] Sizeable knowledge gaps preclude the

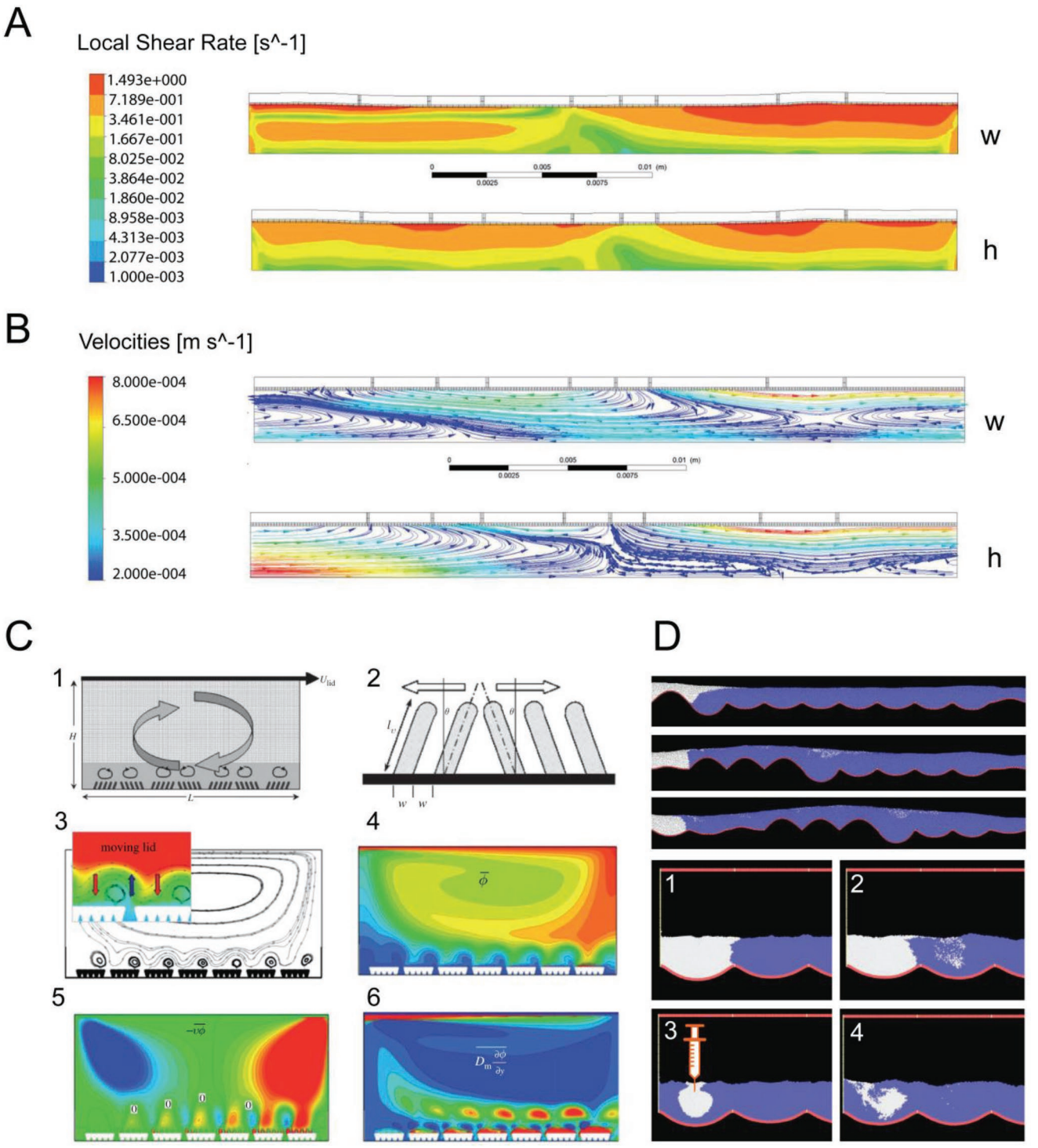

Figure 8. Examples of in silico models used to represent the human gut. A,B) CFD simulation from a rabbit colon model by Fullard et al.;[151b] both images refer to a stretching motion of the colon. A) The shear rates and B) the velocities streamline, both for two different fluids simulations: water (w) and honey (h). (A,B) Adapted with permission.[151b] Copyright 2014, The Royal Society of Chemistry. C) Mathematical model developed by Wang et al.[152a] where 1–2) illustrate the principles of their model in which micro- and macromixing interact; 2) shows a group of villi and the type of motion used in their approach; 3) shows the streamlines; and 4–6) the results of the simulations, respectively, isocontours of molecular concentration, concentration flux by advection, and by diffusion. Reproduced with permission.[152a] Copyright 2010, The Royal Society. D) The top three images are of a simulation of the peristaltic waves moving along the DCM in vitro colon in the mathematical model developed by Alexiadis et al.[154] 1–4) Mixing before and after three waves of the fluid (blue) and tracer (gray) of a 1–2) same or 3–4) different viscosity. Adapted with permission.[154] Copyright 2017, Elsevier.

Table 3. Comparison between different models of the human intestine.

Models	Type	Ethical requirements	Intestinal tissues and cells	Outputs	Benefits	Limitations
Animal	Small animals	✓	Tissue/body cells can be isolated from intestinal tissue	Physiological and mechanism data of disease and treatments Microbes and gut–brain axis studies	Easy genetic manipulation	Replicability issues Require trained personnel
	Large animals	✓			Larger body size Anatomically and genetically similar to humans	High cost Require trained personnel Ethical concerns
In vitro	Static 2D cell culture Transwell devices	Only for patient-derived cells	Enterocytes, goblet, macrophages	Effects of food and drugs (e.g., anti-inflammatory, antioxidant) Absorption and permeability Cytotoxicity	Standardized across labs	Simplified representation by cells
	Microfluidic IsOC	Only for patient-derived cells	Enterocytes, goblet, macrophages.	Effects of food and drugs Absorption and permeability Cytotoxicity Host–microbial interface Crosstalk between different organs	Physiology closer to in vivo Faster cell polarization Intestinal peristalsis contribution	Simplified representation by cells Still to be standardized across labs (there is not one IOC only) Suitability of materials
	3D scaffolds	Only for patient-derived cells	Enterocytes, goblet, myofibroblasts	Absorption and permeability (porous scaffolds) Host–microbial interface	Cell phenotype closer to in vivo Improved bacteria invasion and specific adhesion Can be used under microfluidic perfusion	Simplified representation by cells Support that requires extra material (e.g., close environment for cells) Suitability of materials
	Macromodels	Yes for human fecal samples	Microbiota, mucin-coated supports	Colon-related studies on patient-derived microbiota Fermentation of nutrients and pharmaceuticals	Replicability Specific microbiota compositions Single-patient studies	Microbiota stabilization period needed before experiments Not available to all laboratories Does not consider intestinal absorption Some systems lack peristalsis and dialysis Large space required for the setup Can be costly
In silico	Simulations or CFD	May require ethics for patients' data and privacy	Can model tissue and cellular behaviors	Food and drug structure effects Absorption and permeability, metabolism Prediction of behaviors and dependency between different parameters	Intestinal peristalsis contribution Can be adapted to different geometrical features of the intestine (e.g., children or elderly patients)	Need to know well: transport phenomena and physiology contributions Does not take into account patients' genetic background and response

complete metabolic reconstruction of an organism based on its genome alone. For instance, the genome is a static representation of an organism's total functional capacity; determining from here what it actually does in a given context is nontrivial. Individual organism GSMs tend to be highly complex, and the GSM for the widely employed K-12 *E. coli* strain comprises 3000 reactions and 1200 metabolites.[162] Modeling complex, dynamic (nonsteady state) communities of microorganisms using GSMs remains highly challenging.

The power of modeling stems from an unrestricted capacity to manipulate and measure. However, this is arguably also its greatest challenge—in vivo and in vitro, physics is free. The extent to which models are instructive of reality depends on how well critical system elements, which may be unknown, are captured; the (relevant) rules of physics must be encoded. With sufficient real world data, model accuracy can be accessed through emerging calibration techniques.[163] This is particularly pertinent for highly predictive models aiming to facilitate personalized medicine,[164] wherein a model tailored to a given individual is used to prototype putative intervention strategies. Model dynamics are specified through parameters describing, e.g., rates, population sizes or molecular expression

levels, or probabilities. Where possible, such parameter values can be experimentally ascertained or extracted from literature. Where this is not possible, owing to either the model's abstract nature or its articulation of dynamics not amenable to experimentation, calibration or "fitting" against in vivo and in vitro data is warranted.[165]

9. Conclusions

This Progress Report has discussed the different technologies used to model the gut, which are applicable to modeling disease, disease treatment, as well as diet and food consumption. An overview was given for the advantages and limitations of different intestinal models and the summary of this discussion is provided in **Table 3**.

The physiological and function of the human gut are complex and reliant on several factors including cell types, genetics, the immune system, and disease state. Different types of large and small animal models have been developed for studying the impact of food and nutrition on diseases associated with the gastric system. Such work is a necessary precursor to clinical trials. Cell culture models have been developed to closely represent the features of the human gut. Preference is given to those cell lines that most faithfully represent the in vivo conditions, although there is a scope for greater exploration of mucin expression in these lines. Concomitantly, various in vitro models have been designed to circumvent the challenges of animal models such as ethical constraints, high cost, and physiological differences with humans. These models provide lower cost methods for investigating the direct effects of foods and insights into disease mechanism.

The physiological conditions recreated within the IsOC allow a faster differentiation of the epithelial cell monolayers, and a more accurate representation of the gut architecture. Aside from the lower consumption of reagents and cell number used, the integration of other tools and sensors on-chip, whereas possible, makes IsOC more competitive if compared with the standard cell culture, as analysis can often be carried in situ. Furthermore, IsOC can be designed according to a study needs, connecting multiple organs together for cross-talk and metabolism-related studies. As the field advances, the incorporation of microfabricated or 3D printed scaffolds and gut microbiota are areas of active research. Both macro- and micromodels are readily computer controlled, enabling precision in study execution.

In silico models can be used to refine experimental model systems. In the case of microfluidics, CFD simulations or other methodologies (e.g., finite element analysis) are often used to predict the optimal geometry to be adopted with the aim of providing a uniform shear stress to the cellular layer. Consequently, the flow rates to the microchannels can be selected to guarantee the required conditions. In silico models can lead to major insights on the gut physiology and motility.

A major limitation of the field is the focus on single systems and debate over the relative advantages and disadvantages of such systems. This Progress Report highlights the various strengths of the different gut models and it is suggested that better co-ordination between research groups utilizing different models may yield greater insights into gut function. Ultimately, however, no model system can completely replace the need for clinical/human studies. Even the most sophisticated preclinical animal models do not recapitulate all the components of human intestinal physiology and function, yet each system possesses unique features enabling the exploration of different diseases in the gastric system. The complementary integration of the different models summarized in this Progress Report could yield substantive additional insights into the complex physiology of the human gut.

Acknowledgements

The authors acknowledge the financial support from the Australian Research Council Grant Nos. IC140100026 and DP 270102931 as well as the University of Sydney for establishing Centre for Advanced Food Enginomics. C.A.M.F. acknowledges the Faculty of Engineering of the University of Sydney for her scholarship.

Conflict of Interest

The authors declare no conflict of interest.

Keywords

gut models, human intestine, inflammatory bowel disease, intestine-on-a-chip, microfluidics

Received: July 22, 2019
Revised: August 30, 2019
Published online: October 8, 2019

[1] a) T. K. Soderborg, J. E. Friedman, *Microb. Cell* **2019**, *6*, 102; b) M. Maguire, G. Maguire, *Rev. Neurosci.* **2019**, *30*, 179.
[2] a) M. C. Houser, M. G. Tansey, *npj Parkinson's Dis.* **2017**, *3*, 3; b) A. I. Petra, S. Panagiotidou, E. Hatziagelaki, J. M. Stewart, P. Conti, T. C. Theoharides, *Clin. Ther.* **2015**, *37*, 984; c) J. I. Campos Acuña, D. Elgueta, R. Pacheco, *Front. Immunol.* **2019**, *10*, 239.
[3] a) B. C. Olendzki, T. D. Silverstein, G. M. Persuitte, Y. Ma, K. R. Baldwin, D. Cave, *Nutr. J.* **2014**, *13*, 5; b) A. C. Brown, S. D. Rampertab, G. E. Mullin, *Expert Rev. Gastroenterol. Hepatol.* **2011**, *5*, 411; c) J. D. Lewis, M. T. Abreu, *Gastroenterology* **2017**, *152*, 398.
[4] a) T. L. A. Nguyen, S. Vieira-Silva, A. Liston, J. Raes, *Dis. Models Mech.* **2015**, *8*, 1; b) M.-C. Arrieta, J. Walter, B. B. Finlay, *Cell Host Microbe* **2016**, *19*, 575.
[5] Y. Chen, Y. Lin, K. M. Davis, Q. Wang, J. Rnjak-Kovacina, C. Li, R. R. Isberg, C. A. Kumamoto, J. Mecsas, D. L. Kaplan, *Sci. Rep.* **2015**, *5*, 13708.
[6] J.-Y. Sun, X. Zhao, W. R. Illeperuma, O. Chaudhuri, K. H. Oh, D. J. Mooney, J. J. Vlassak, Z. Suo, *Nature* **2012**, *489*, 133.
[7] a) S. N. Bhatia, D. E. Ingber, *Nat. Biotechnol.* **2014**, *32*, 760; b) A. Van Den Berg, C. L. Mummery, R. Passier, A. D. Van der Meer, *Lab Chip* **2019**, *19*, 198.
[8] a) B. D. Simons, H. Clevers, *Exp. Cell Res.* **2011**, *317*, 2719; b) V. Balbi, P. Ciarletta, *J. R. Soc., Interface* **2013**, *10*, 20130109.
[9] a) T. K. Noah, B. Donahue, N. F. Shroyer, *Exp. Cell Res.* **2011**, *317*, 2702; b) L. G. van der Flier, H. Clevers, *Annu. Rev. Physiol.* **2009**, *71*, 241.

[10] R. Latorre, C. Sternini, R. De Giorgio, B. Greenwood-Van Meerveld, *Neurogastroenterol. Motil.* **2016**, *28*, 620.
[11] S. Vaishnava, M. Yamamoto, K. M. Severson, K. A. Ruhn, X. Yu, O. Koren, R. Ley, E. K. Wakeland, L. V. Hooper, *Science* **2011**, *334*, 255.
[12] M. E. Johansson, H. Sjovall, G. C. Hansson, *Nat. Rev. Gastroenterol. Hepatol.* **2013**, *10*, 352.
[13] C. Abraham, J. H. Cho, *N. Engl. J. Med.* **2009**, *361*, 2066.
[14] a) K. Makki, E. C. Deehan, J. Walter, F. Backhed, *Cell Host Microbe* **2018**, *23*, 705; b) D. A. Winer, H. Luck, S. Tsai, S. Winer, *Cell Metab.* **2016**, *23*, 413; c) D. A. Winer, S. Winer, H. J. Dranse, T. K. Lam, *J. Clin. Invest.* **2017**, *127*, 33.
[15] M. Akdis, *Curr. Opin. Immunol.* **2006**, *18*, 738.
[16] S. R. Gill, M. Pop, R. T. Deboy, P. B. Eckburg, P. J. Turnbaugh, B. S. Samuel, J. I. Gordon, D. A. Relman, C. M. Fraser-Liggett, K. E. Nelson, *Science* **2006**, *312*, 1355.
[17] H. J. Flint, K. P. Scott, P. Louis, S. H. Duncan, *Nat. Rev. Gastroenterol. Hepatol.* **2012**, *9*, 577.
[18] A. V. Vila, F. Imhann, V. Collij, S. A. Jankipersadsing, T. Gurry, Z. Mujagic, A. Kurilshikov, M. J. Bonder, X. F. Jiang, E. F. Tigchelaar, J. Dekens, V. Peters, M. D. Voskuil, M. C. Visschedijk, H. M. van Dullemen, D. Keszthelyi, M. A. Swertz, L. Franke, R. Alberts, E. A. M. Festen, G. Dijkstra, A. A. M. Masclee, M. H. Hofker, R. J. Xavier, E. J. Alm, J. Fu, C. W. Section, D. M. A. E. J. Section, A. Zhernakova, R. K. Weersma, *Sci. Transl. Med.* **2018**, *10*, eaap8914.
[19] R. K. Singh, H. W. Chang, D. Yan, K. M. Lee, D. Ucmak, K. Wong, M. Abrouk, B. Farahnik, M. Nakamura, T. H. Zhu, T. Bhutani, W. Liao, *J. Transl. Med.* **2017**, *15*, 73.
[20] T. Sen, C. R. Cawthon, B. T. Ihde, A. Hajnal, P. M. DiLorenzo, C. B. de La Serre, K. Czaja, *Physiol. Behav.* **2017**, *173*, 305.
[21] a) A. Geremia, P. Biancheri, P. Allan, G. R. Corazza, A. Di Sabatino, *Autoimmun. Rev.* **2014**, *13*, 3; b) W. Strober, I. J. Fuss, R. S. Blumberg, *Annu. Rev. Immunol.* **2002**, *20*, 495.
[22] P. M. Smith, M. R. Howitt, N. Panikov, M. Michaud, C. A. Gallini, M. Bohlooly-y, J. N. Glickman, W. S. Garrett, *Science* **2013**, *341*, 569.
[23] A. Khosravi, S. K. Mazmanian, *Curr. Opin. Microbiol.* **2013**, *16*, 221.
[24] a) E. M. Brown, M. Sadarangani, B. B. Finlay, *Nat. Immunol.* **2013**, *14*, 660; b) G. Cammarota, G. Ianiro, R. Cianci, S. Sibbo, A. Gasbarrini, D. Curro, *Pharmacol. Ther.* **2015**, *149*, 191; c) K. Fyderek, M. Strus, K. Kowalska-Duplaga, T. Gosiewski, A. Wedrychowicz, U. Jedynak-Wasowicz, M. Sladek, S. Pieczarkowski, P. Adamski, P. Kochan, P. B. Heczko, *World J. Gastroenterol.* **2009**, *15*, 5287; d) N. Kamada, S. U. Seo, G. Y. Chen, G. Nunez, *Nat. Rev. Immunol.* **2013**, *13*, 321; e) A. D. Kostic, R. J. Xavier, D. Gevers, *Gastroenterology* **2014**, *146*, 1489; f) C. Manichanh, N. Borruel, F. Casellas, F. Guarner, *Nat. Rev. Gastroenterol. Hepatol.* **2012**, *9*, 599; g) C. Reiff, D. Kelly, *Int. J. Med. Microbiol.* **2010**, *300*, 25.
[25] a) A. Forbes, J. Escher, X. Hebuterne, S. Klek, Z. Krznaric, S. Schneider, R. Shamir, K. Stardelova, N. Wierdsma, A. E. Wiskin, S. C. Bischoff, *Clin. Nutr.* **2017**, *36*, 321; b) S. Massironi, R. E. Rossi, F. A. Cavalcoli, S. Della Valle, M. Fraquelli, D. Conte, *Clin. Nutr.* **2013**, *32*, 904; c) D. D. Mijac, G. L. J. Jankovic, J. Jorga, M. N. Krstic, *Eur. J. Intern. Med.* **2010**, *21*, 315.
[26] a) L. S. Conklin, M. Oliva-Hemker, *Expert Rev. Gastroenterol. Hepatol.* **2010**, *4*, 305; b) D. P. Mallon, D. L. Suskind, *Nutr. Clin. Pract.* **2010**, *25*, 335; c) K. Vagianos, S. Bector, J. McConnell, C. N. Bernstein, *JPEN, J. Parenter. Enteral Nutr.* **2007**, *31*, 311.
[27] a) J. H. Cho, *Nat. Rev. Immunol.* **2008**, *8*, 458; b) B. Khor, A. Gardet, R. J. Xavier, *Nature* **2011**, *474*, 307; c) T. C. Liu, T. S. Stappenbeck, *Annu. Rev. Pathol.: Mech. Dis.* **2016**, *11*, 127; d) S. C. Ng, C. N. Bernstein, M. H. Vatn, P. L. Lakatos, E. V. Loftus Jr., C. Tysk, C. O'Morain, B. Moum, J. F. Colombel, *Gut* **2013**, *62*, 630.
[28] a) D. T. Rubin, S. Becker, M. Siegler, *Gastroenterol. Hepatol.* **2014**, *10*, 37; b) C. M. Weaver, J. W. Miller, *Nutr. Rev.* **2017**, *75*, 491.
[29] a) L. M. Sollid, F. E. Johansen, *PLoS Med.* **2008**, *5*, e198; b) R. W. Engelman, W. G. Kerr, *Methods Mol. Biol.* **2012**, *900*, 433.
[30] a) K. Praengam, Y. Sahasakul, P. Kupradinun, S. Sakarin, W. Sanitchua, A. Rungsipipat, K. Rattanapinyopituk, P. Angkasekwinai, K. Changsri, W. Mhuantong, S. Tangphatsornruang, S. Tuntipopipat, *Food Funct.* **2017**, *8*, 4630; b) B. Chassaing, J. D. Aitken, M. Malleshappa, M. Vijay-Kumar, *Curr. Protoc. Immunol.* **2014**, *104*, 15.25.1.
[31] a) A. Mizoguchi, E. Mizoguchi, A. K. Bhan, *Inflammatory Bowel Dis.* **2003**, *9*, 246; b) S. Nell, S. Suerbaum, C. Josenhans, *Nat. Rev. Microbiol.* **2010**, *8*, 564; c) N. Elguezabal, S. Chamorro, E. Molina, J. M. Garrido, A. Izeta, L. Rodrigo, R. A. Juste, *Gut Pathog.* **2012**, *4*, 6; d) J. L. Coombes, N. J. Robinson, K. J. Maloy, H. H. Uhlig, F. Powrie, *Immunol. Rev.* **2005**, *204*, 184.
[32] Mouse Genome Sequencing Consortium, R. H. Waterston, K. Lindblad-Toh, E. Birney, J. Rogers, J. F. Abril, P. Agarwal, R. Agarwala, R. Ainscough, M. Alexandersson, P. An, S. E. Antonarakis, J. Attwood, R. Baertsch, J. Bailey, K. Barlow, S. Beck, E. Berry, B. Birren, T. Bloom, P. Bork, M. Botcherby, N. Bray, M. R. Brent, D. G. Brown, S. D. Brown, C. Bult, J. Burton, J. Butler, R. D. Campbell, P. Carninci, S. Cawley, F. Chiaromonte, A. T. Chinwalla, D. M. Church, M. Clamp, C. Clee, F. S. Collins, L. L. Cook, R. R. Copley, A. Coulson, O. Couronne, J. Cuff, V. Curwen, T. Cutts, M. Daly, R. David, J. Davies, K. D. Delehaunty, J. Deri, E. T. Dermitzakis, C. Dewey, N. J. Dickens, M. Diekhans, S. Dodge, I. Dubchak, D. M. Dunn, S. R. Eddy, L. Elnitski, R. D. Emes, P. Eswara, E. Eyras, A. Felsenfeld, G. A. Fewell, P. Flicek, K. Foley, W. N. Frankel, L. A. Fulton, R. S. Fulton, T. S. Furey, D. Gage, R. A. Gibbs, G. Glusman, S. Gnerre, N. Goldman, L. Goodstadt, D. Grafham, T. A. Graves, E. D. Green, S. Gregory, R. Guigo, M. Guyer, R. C. Hardison, D. Haussler, Y. Hayashizaki, L. W. Hillier, A. Hinrichs, W. Hlavina, T. Holzer, F. Hsu, A. Hua, T. Hubbard, A. Hunt, I. Jackson, D. B. Jaffe, L. S. Johnson, M. Jones, T. A. Jones, A. Joy, M. Kamal, E. K. Karlsson, D. Karolchik, A. Kasprzyk, J. Kawai, E. Keibler, C. Kells, W. J. Kent, A. Kirby, D. L. Kolbe, I. Korf, R. S. Kucherlapati, E. J. Kulbokas, D. Kulp, T. Landers, J. P. Leger, S. Leonard, I. Letunic, R. Levine, J. Li, M. Li, C. Lloyd, S. Lucas, B. Ma, D. R. Maglott, E. R. Mardis, L. Matthews, E. Mauceli, J. H. Mayer, M. McCarthy, W. R. McCombie, S. McLaren, K. McLay, J. D. McPherson, J. Meldrim, B. Meredith, J. P. Mesirov, W. Miller, T. L. Miner, E. Mongin, K. T. Montgomery, M. Morgan, R. Mott, J. C. Mullikin, D. M. Muzny, W. E. Nash, J. O. Nelson, M. N. Nhan, R. Nicol, Z. Ning, C. Nusbaum, M. J. O'Connor, Y. Okazaki, K. Oliver, E. Overton-Larty, L. Pachter, G. Parra, K. H. Pepin, J. Peterson, P. Pevzner, R. Plumb, C. S. Pohl, A. Poliakov, T. C. Ponce, C. P. Ponting, S. Potter, M. Quail, A. Reymond, B. A. Roe, K. M. Roskin, E. M. Rubin, A. G. Rust, R. Santos, V. Sapojnikov, B. Schultz, J. Schultz, M. S. Schwartz, S. Schwartz, C. Scott, S. Seaman, S. Searle, T. Sharpe, A. Sheridan, R. Shownkeen, S. Sims, J. B. Singer, G. Slater, A. Smit, D. R. Smith, B. Spencer, A. Stabenau, N. Stange-Thomann, C. Sugnet, M. Suyama, G. Tesler, J. Thompson, D. Torrents, E. Trevaskis, J. Tromp, C. Ucla, A. Ureta-Vidal, J. P. Vinson, A. C. Von Niederhausern, C. M. Wade, M. Wall, R. J. Weber, R. B. Weiss, M. C. Wendl, A. P. West, K. Wetterstrand, R. Wheeler, S. Whelan, J. Wierzbowski, D. Willey, S. Williams, R. K. Wilson, E. Winter, K. C. Worley, D. Wyman, S. Yang, S. P. Yang, E. M. Zdobnov, M. C. Zody, E. S. Lander, *Nature* **2002**, *420*, 520.
[33] a) K. Abnous, S. P. J. Brooks, J. Kwan, F. Matias, J. Green-Johnson, L. B. Selinger, M. Thomas, M. Kalmokoff, *J. Nutr.* **2009**, *139*, 2024; b) M. Kalmokoff, B. Zwicker, M. O'Hara, F. Matias, J. Green,

P. Shastri, J. Green-Johnson, S. P. J. Brooks, *J. Appl. Microbiol.* **2013**, *114*, 1516.
[34] a) R. E. Hammer, S. D. Maika, J. A. Richardson, J. P. Tang, J. D. Taurog, *Cell* **1990**, *63*, 1099; b) H. C. Rath, H. H. Herfarth, J. S. Ikeda, W. B. Grenther, T. E. Hamm, E. Balish, J. D. Taurog, R. E. Hammer, K. H. Wilson, R. B. Sartor, *J. Clin. Invest.* **1996**, *98*, 945.
[35] W. Morales, M. Pimentel, L. Hwang, D. Kunkel, V. Pokkunuri, B. Basseri, K. Low, H. L. Wang, J. L. Conklin, C. Chang, *Dig. Dis. Sci.* **2011**, *56*, 2575.
[36] a) E. M. Bautista, C. Nfon, G. S. Ferman, W. T. Golde, *Vet. Immunol. Immunopathol.* **2007**, *115*, 56; b) X. Lu, W. X. Fu, Y. R. Luo, X. D. Ding, J. P. Zhou, Y. Liu, J. F. Liu, Q. Zhang, *BMC Genomics* **2012**, *13*, 488; c) Q. Zhang, G. Widmer, S. Tzipori, *Gut Microbes* **2013**, *4*, 193; d) L. Scharek, J. Guth, K. Reiter, K. D. Weyrauch, D. Taras, P. Schwerk, P. Schierack, M. F. Schmidt, L. H. Wieler, K. Tedin, *Vet. Immunol. Immunopathol.* **2005**, *105*, 151; e) N. Foster, M. A. Lovell, K. L. Marston, S. D. Hulme, A. J. Frost, P. Bland, P. A. Barrow, *Infect. Immun.* **2003**, *71*, 2182.
[37] a) E. M. Walters, E. Wolf, J. J. Whyte, J. Mao, S. Renner, H. Nagashima, E. Kobayashi, J. G. Zhao, K. D. Wells, J. K. Critser, L. K. Riley, R. S. Prather, *BMC Med. Genomics* **2012**, *5*, 55; b) J. K. Patterson, X. G. Lei, D. D. Miller, *Exp. Biol. Med.* **2008**, *233*, 651.
[38] L. P. Coelho, J. R. Kultima, P. I. Costea, C. Fournier, Y. Pan, G. Czarnecki-Maulden, M. R. Hayward, S. K. Forslund, T. S. B. Schmidt, P. Descombes, J. R. Jackson, Q. Li, P. Bork, *Microbiome* **2018**, *6*, 72.
[39] a) A. Kathrani, H. Lee, C. White, B. Catchpole, A. Murphy, A. German, D. Werling, K. Allenspach, *Vet. Immunol. Immunopathol.* **2014**, *161*, 32; b) M. Cerquetella, A. Spaterna, F. Laus, B. Tesei, G. Rossi, E. Antonelli, V. Villanacci, G. Bassotti, *World J. Gastroenterol.* **2010**, *16*, 1050.
[40] K. R. Amato, C. J. Yeoman, G. Cerda, C. A. Schmitt, J. D. Cramer, M. E. Miller, A. Gomez, T. R. Turner, B. A. Wilson, R. M. Stumpf, K. E. Nelson, B. A. White, R. Knight, S. R. Leigh, *Microbiome* **2015**, *3*, 53.
[41] a) M. E. Coors, J. J. Glover, E. T. Juengst, J. M. Sikela, *Nat. Rev. Genet.* **2010**, *11*, 658; b) M. Ideland, *J. Med. Ethics* **2009**, *35*, 258.
[42] a) G. Gabella, *Neuroscience* **1987**, *22*, 737; b) P. Rangan, I. Choi, M. Wei, G. Navarrete, E. Guen, S. Brandhorst, N. Enyati, G. Pasia, D. Maesincee, V. Ocon, M. Abdulridha, V. D. Longo, *Cell Rep.* **2019**, *26*, 2704.
[43] D. L. Miller, *Am. J. Dig. Dis.* **1971**, *16*, 247.
[44] a) L. M. Gonzalez, A. J. Moeser, A. T. Blikslager, *Transl. Res.* **2015**, *166*, 12; b) S. F. Vaessen, M. M. van Lipzig, R. H. Pieters, C. A. Krul, H. M. Wortelboer, E. van de Steeg, *Drug Metab. Dispos.* **2017**, *45*, 353; c) Y. Xiao, H. Yan, H. Diao, B. Yu, J. He, J. Yu, P. Zheng, X. Mao, Y. Luo, D. Chen, *Sci. Rep.* **2017**, *7*, 3224; d) S. N. Heinritz, R. Mosenthin, E. Weiss, *Nutr. Res. Rev.* **2013**, *26*, 191.
[45] D. B. Paulsen, K. K. Buddington, R. K. Buddington, *Am. J. Vet. Res.* **2003**, *64*, 618.
[46] R. Nagpal, C. A. Shively, S. A. Appt, T. C. Register, K. T. Michalson, M. Z. Vitolins, H. Yadav, *Front. Nutr.* **2018**, *5*, 28.
[47] K. E. Barrett, S. M. Barman, S. Boitano, H. Brooks, *Ganong's Review of Medical Physiology*, 23rd ed., McGraw-Hill Medical, New York, NY **2009**.
[48] X.-D. Bu, N. Li, X.-Q. Tian, P.-L. Huang, *Tissue Cell* **2011**, *43*, 201.
[49] B. J.-W. van Klinken, E. Oussoren, J.-J. Weenink, G. J. Strous, H. A. Büller, J. Dekker, A. W. Einerhand, *Glycoconjugate J.* **1996**, *13*, 757.
[50] C. Pontier, J. Pachot, R. Botham, B. Lenfant, P. Arnaud, *J. Pharm. Sci.* **2001**, *90*, 1608.
[51] Y. Niv, J. C. Byrd, S. B. Ho, R. Dahiya, Y. S. Kim, *Int. J. Cancer* **1992**, *50*, 147.
[52] P. Schierack, M. Nordhoff, M. Pollmann, K. D. Weyrauch, S. Amasheh, U. Lodemann, J. Jores, B. Tachu, S. Kleta, A. Blikslager, *Histochem. Cell Biol.* **2006**, *125*, 293.
[53] a) C. L. Kinlough, P. A. Poland, S. J. Gendler, P. E. Mattila, D. Mo, O. A. Weisz, R. P. Hughey, *J. Biol. Chem.* **2011**, *286*, 39072; b) J. Lavelle, H. Negrete, P. Poland, C. Kinlough, S. Meyers, R. Hughey, M. Zeidel, *Am. J. Physiol.: Cell Physiol.* **1997**, *273*, C67.
[54] J. Fogh, T. Orfeo, J. Tiso, F. E. Sharkey, *Pathobiology* **1979**, *47*, 136.
[55] T. Lea, in *The Impact of Food Bioactives on Health: In Vitro and Ex Vivo Models* (Eds: K. Verhoeckx, P. Cotter, I. Lopez-Exposito, C. Kleiveland, T. Lea, A. Mackie, T. Requena, D. Swiatecka, H. Wichers), Springer, Cham, Switzerland **2015**, (Ch. 10) pp. 103–111, (https://doi.org/10.1007/978-3-319-16104-4_10).
[56] a) P. Artursson, J. Karlsson, *Biochem. Biophys. Res. Commun.* **1991**, *175*, 880; b) K. Cheng, C. Li, A. S. Uss, *Expert Opin. Drug Metab. Toxicol.* **2008**, *4*, 581; c) I. Hubatsch, E. G. Ragnarsson, P. Artursson, *Nat. Protoc.* **2007**, *2*, 2111.
[57] a) S. Gratz, Q. Wu, H. El-Nezami, R. Juvonen, H. Mykkänen, P. Turner, *Appl. Environ. Microbiol.* **2007**, *73*, 3958; b) Y. Li, C. Zhang, L. Liu, Y. Gong, Y. Xie, Y. Cao, *Toxicol. Mech. Methods* **2018**, *28*, 167.
[58] a) A. Malapert, V. R. Tomao, O. Dangles, E. Reboul, *J. Agric. Food Chem.* **2018**, *66*, 4614; b) N. Andrade, J. R. Araujo, A. Correia-Branco, J. V. Carletti, F. Martel, *J. Funct. Foods* **2017**, *36*, 429; c) R. Sánchez-Vioque, O. Santana-Méridas, M. Polissiou, J. Vioque, K. Astraka, M. Alaiz, D. Herraiz-Peñalver, P. A. Tarantilis, J. Girón-Calle, *J. Funct. Foods* **2016**, *24*, 18; d) S. Maccaferri, A. Klinder, P. Brigidi, P. Cavina, A. Costabile, *Appl. Environ. Microbiol.* **2012**, *78*, 956.
[59] M. D. Peterson, M. S. Mooseker, *J. Cell Sci.* **1992**, *102*, 581.
[60] D. Martínez-Maqueda, B. Miralles, I. Recio, in *The Impact of Food Bioactives on Health: In Vitro and Ex Vivo Models* (Eds: K. Verhoeckx, P. Cotter, I. Lopez-Exposito, C. Kleiveland, T. Lea, A. Mackie, T. Requena, D. Swiatecka, H. Wichers), Springer, Cham, Switzerland **2015**, p. 113, Ch. 11.
[61] G. J. Mahler, M. L. Shuler, R. P. Glahn, *J. Nutr. Biochem.* **2009**, *20*, 494.
[62] I. Lozoya-Agullo, F. Araújo, I. González-Álvarez, M. Merino-Sanjuán, M. González-Álvarez, M. Bermejo, B. Sarmento, *Mol. Pharmaceutics* **2017**, *14*, 1264.
[63] a) M. Gagnon, A. Z. Berner, N. Chervet, C. Chassard, C. Lacroix, *J. Microbiol. Methods* **2013**, *94*, 274; b) J. M. Laparra, Y. Sanz, *Lett. Appl. Microbiol.* **2009**, *49*, 695; c) J. Naughton, G. Duggan, B. Bourke, M. Clyne, *Gut Microbes* **2014**, *5*, 48.
[64] H. Berschneider, *Gastroenterology* **1989**, *96*, A41.
[65] M. M. Geens, T. A. Niewold, *Cytotechnology* **2011**, *63*, 415.
[66] M. J. Cho, D. P. Thompson, C. T. Cramer, T. J. Vidmar, J. F. Scieszka, *Pharm. Res.* **1989**, *6*, 71.
[67] F. Antunes, F. Andrade, D. Ferreira, H. Morck Nielsen, B. Sarmento, *Curr. Drug Metab.* **2013**, *14*, 4.
[68] W. S. Putnam, L. Pan, K. Tsutsui, L. Takahashi, L. Z. Benet, *Pharm. Res.* **2002**, *19*, 27.
[69] Y. Takahashi, S. Sato, Y. Kurashima, T. Yamamoto, S. Kurokawa, Y. Yuki, N. Takemura, S. Uematsu, C.-Y. Lai, M. Otsu, *Stem Cell Rep.* **2018**, *10*, 314.
[70] N. Gjorevski, N. Sachs, A. Manfrin, S. Giger, M. E. Bragina, P. Ordóñez-Morán, H. Clevers, M. P. Lutolf, *Nature* **2016**, *539*, 560.
[71] a) A. Sin, K. C. Chin, M. F. Jamil, Y. Kostov, G. Rao, M. L. Shuler, *Biotechnol. Prog.* **2004**, *20*, 338; b) R. Khamsi, *Nature* **2005**, *435*, 12.
[72] Pharmaceutical Research and Manufacturers of America, *2016 Biopharmaceutical Research Industry Profile*, PhRMA, Washington, DC **2016**.

[73] R. K. Harrison, *Nat. Rev. Drug Discovery* **2016**, *15*, 817.
[74] a) K. Brøsen, C. Funck-Brentano, H. K. Kroemer, M. Pirmohamed, M. Schwab, *Lancet* **2017**, *389*, 156; b) J. Randerson, *Nature* **2016**, https://doi.org/10.1038/nature.2016.21190; c) E. Callaway, D. Butler, *Nature* **2016**, *529*, 263.
[75] H. Y. Tan, S. Trier, U. L. Rahbek, M. Dufva, J. P. Kutter, T. L. Andresen, *PLoS One* **2018**, *13*, e0197101.
[76] H. Kimura, T. Yamamoto, H. Sakai, Y. Sakai, T. Fujii, *Lab Chip* **2008**, *8*, 741.
[77] a) M. Shuler, *US 7288405 B2*, **2007**; b) J. H. Sung, C. Kam, M. L. Shuler, *Lab Chip* **2010**, *10*, 446.
[78] H. Lee, D. S. Kim, S. K. Ha, I. Choi, J. M. Lee, J. H. Sung, *Biotechnol. Bioeng.* **2017**, *114*, 432.
[79] a) K. Kulthong, *RSC Adv.* **2018**, *8*, 32440; b) K. Pocock, L. Delon, V. Bala, S. Rao, C. Priest, C. Prestidge, B. Thierry, *ACS Biomater. Sci. Eng.* **2017**, *3*, 951.
[80] Y. Imura, Y. Asano, K. Sato, E. Yoshimura, *Anal. Sci.* **2009**, *25*, 1403.
[81] a) Q. Ramadan, H. Jafarpoorchekab, C. Huang, P. Silacci, S. Carrara, G. Koklu, J. Ghaye, J. Ramsden, C. Ruffert, G. Vergeres, M. A. Gijs, *Lab Chip* **2013**, *13*, 196; b) G. Vergeres, B. Bogicevic, C. Buri, S. Carrara, M. Chollet, L. Corbino-Giunta, L. Egger, D. Gille, K. Kopf-Bolanz, K. Laederach, R. Portmann, Q. Ramadan, J. Ramsden, F. Schwander, P. Silacci, B. Walther, M. Gijs, *Br. J. Nutr.* **2012**, *108*, 762.
[82] C. Huang, Q. Ramadan, J. B. Wacker, H. C. Tekin, C. Ruffert, G. Vergeres, P. Silacci, M. A. M. Gijs, *RSC Adv.* **2014**, *4*, 52887.
[83] A. Choe, S. K. Ha, I. Choi, N. Choi, J. H. Sung, *Biomed. Microdevices* **2017**, *19*, 4.
[84] Y. Imura, K. Sato, E. Yoshimura, *Anal. Chem.* **2010**, *82*, 9983.
[85] R. Villenave, S. Q. Wales, T. Hamkins-Indik, E. Papafragkou, J. C. Weaver, T. C. Ferrante, A. Bahinski, C. A. Elkins, M. Kulka, D. E. Ingber, *PLoS One* **2017**, *12*, e0169412.
[86] S. Jalili-Firoozinezhad, R. Prantil-Baun, A. Jiang, R. Potla, T. Mammoto, J. C. Weaver, T. C. Ferrante, H. J. Kim, J. M. S. Cabral, O. Levy, D. E. Ingber, *Cell Death Dis.* **2018**, *9*, 223.
[87] M. B. Esch, G. J. Mahler, T. Stokol, M. L. Shuler, *Lab Chip* **2014**, *14*, 3081.
[88] Q. Ramadan, L. Jing, *Biomed. Microdevices* **2016**, *18*, 11.
[89] a) M. Kasendra, A. Tovaglieri, A. Sontheimer-Phelps, S. Jalili-Firooz inezhad, A. Bein, A. Chalkiadaki, W. Scholl, C. Zhang, H. Rickner, C. A. Richmond, H. Li, D. T. Breault, D. E. Ingber, *Sci. Rep.* **2018**, *8*, 2871; b) M. J. Workman, J. P. Gleeson, E. J. Troisi, H. Q. Estrada, S. J. Kerns, C. D. Hinojosa, G. A. Hamilton, S. R. Targan, C. N. Svendsen, R. J. Barrett, *Cell. Mol. Gastroenterol. Hepatol.* **2018**, *5*, 669.
[90] S. R. Merker, J. Weitz, D. E. Stange, *Dev. Biol.* **2016**, *420*, 239.
[91] H. J. Kim, D. Huh, G. Hamilton, D. E. Ingber, *Lab Chip* **2012**, *12*, 2165.
[92] P. Shah, J. V. Fritz, E. Glaab, M. S. Desai, K. Greenhalgh, A. Frachet, M. Niegowska, M. Estes, C. Jager, C. Seguin-Devaux, F. Zenhausern, P. Wilmes, *Nat. Commun.* **2016**, *7*, 11535.
[93] H. J. Kim, H. Li, J. J. Collins, D. E. Ingber, *Proc. Natl. Acad. Sci. USA* **2016**, *113*, E7.
[94] S. Jalili-Firoozinezhad, F. S. Gazzaniga, E. L. Calamari, D. M. Camacho, C. W. Fadel, A. Bein, B. Swenor, B. Nestor, M. J. Cronce, A. Tovaglieri, O. Levy, K. E. Gregory, D. T. Breault, J. M. S. Cabral, D. L. Kasper, R. Novak, D. E. Ingber, *Nat. Biomed. Eng.* **2018**, *3*, 520.
[95] H. J. Kim, D. E. Ingber, *Integr. Biol.* **2013**, *5*, 1130.
[96] S. J. Trietsch, E. Naumovska, D. Kurek, M. C. Setyawati, M. K. Vormann, K. J. Wilschut, H. L. Lanz, A. Nicolas, C. P. Ng, J. Joore, *Nat. Commun.* **2017**, *8*, 262.
[97] Y. Wang, Z. Shao, W. Zheng, Y. Xie, G. Luo, M. Ding, Q. Liang, *Biofabrication* **2019**, *11*, 045001.
[98] W. L. K. Chen, C. Edington, E. Suter, J. J. Yu, J. J. Velazquez, J. G. Velazquez, M. Shockley, E. M. Large, R. Venkataramanan, D. J. Hughes, C. L. Stokes, D. L. Trumper, R. L. Carrier, M. Cirit, L. G. Griffith, D. A. Lauffenburger, *Biotechnol. Bioeng.* **2017**, *114*, 2648.
[99] I. Maschmeyer, T. Hasenberg, A. Jaenicke, M. Lindner, A. K. Lorenz, J. Zech, L. A. Garbe, F. Sonntag, P. Hayden, S. Ayehunie, R. Lauster, U. Marx, E. M. Materne, *Eur. J. Pharm. Biopharm.* **2015**, *95*, 77.
[100] I. Maschmeyer, A. K. Lorenz, K. Schimek, T. Hasenberg, A. P. Ramme, J. Hübner, M. Lindner, C. Drewell, S. Bauer, A. Thomas, *Lab Chip* **2015**, *15*, 2688.
[101] K. Domansky, J. D. Sliz, N. Wen, C. Hinojosa, G. Thompson, J. P. Fraser, T. Hamkins-Indik, G. A. Hamilton, D. Levner, D. E. Ingber, *Microfluid. Nanofluid.* **2017**, *21*, 107.
[102] S. Halldorsson, E. Lucumi, R. Gómez-Sjöberg, R. M. Fleming, *Biosens. Bioelectron.* **2015**, *63*, 218.
[103] a) M. P. Wolf, G. B. Salieb-Beugelaar, P. Hunziker, *Prog. Polym. Sci.* **2018**, *83*, 97; b) A. Gokaltun, M. L. Yarmush, A. Asatekin, O. B. Usta, *Technology* **2017**, *5*, 1.
[104] T. Sato, R. G. Vries, H. J. Snippert, M. van de Wetering, N. Barker, D. E. Stange, J. H. van Es, A. Abo, P. Kujala, P. J. Peters, H. Clevers, *Nature* **2009**, *459*, 262.
[105] a) J. H. Sung, J. Yu, D. Luo, M. L. Shuler, J. C. March, *Lab Chip* **2011**, *11*, 389; b) C. M. Costello, J. Hongpeng, S. Shaffiey, J. Yu, N. K. Jain, D. Hackam, J. C. March, *Biotechnol. Bioeng.* **2014**, *111*, 1222; c) J. Z. Yu, E. Korkmaz, M. I. Berg, P. R. LeDuc, O. B. Ozdoganlar, *Biomaterials* **2017**, *128*, 109.
[106] a) S. R. Caliari, J. A. Burdick, *Nat. Methods* **2016**, *13*, 405; b) S. H. Kim, M. Chi, B. Yi, S. H. Kim, S. Oh, Y. Kim, S. Park, J. H. Sung, *Integr. Biol* **2014**, *6*, 1122; c) C. M. Costello, R. M. Sorna, Y.-L. Goh, I. Cengic, N. K. Jain, J. C. March, *Mol. Pharmaceutics* **2014**, *11*, 2030; d) C. M. Costello, M. B. Phillipsen, L. M. Hartmanis, M. A. Kwasnica, V. Chen, D. Hackam, M. W. Chang, W. E. Bentley, J. C. March, *Sci. Rep.* **2017**, *7*, 12515.
[107] a) C. Norotte, F. S. Marga, L. E. Niklason, G. Forgacs, *Biomaterials* **2009**, *30*, 5910; b) X. Ma, X. Qu, W. Zhu, Y.-S. Li, S. Yuan, H. Zhang, J. Liu, P. Wang, C. S. E. Lai, F. Zanella, G.-S. Feng, F. Sheikh, S. Chien, S. Chen, *Proc. Natl. Acad. Sci. USA* **2016**, *113*, 2206.
[108] T. Jungst, W. Smolan, K. Schacht, T. Scheibel, J. Groll, *Chem. Rev.* **2016**, *116*, 1496.
[109] X. Cui, K. Breitenkamp, M. G. Finn, M. Lotz, D. D. D'Lima, *Tissue Eng., Part A* **2012**, *18*, 1304.
[110] T. Billiet, E. Gevaert, T. De Schryver, M. Cornelissen, P. Dubruel, *Biomaterials* **2014**, *35*, 49.
[111] N. E. Fedorovich, I. Swennen, J. Girones, L. Moroni, C. A. van Bl itterswijk, E. Schacht, J. Alblas, W. J. A. Dhert, *Biomacromolecules* **2009**, *10*, 1689.
[112] X. Wang, Y. Yan, Y. Pan, Z. Xiong, H. Liu, J. Cheng, F. Liu, F. Lin, R. Wu, R. Zhang, Q. Lu, *Tissue Eng.* **2006**, *12*, 83.
[113] Y. Yan, X. Wang, Y. Pan, H. Liu, J. Cheng, Z. Xiong, F. Lin, R. Wu, R. Zhang, Q. Lu, *Biomaterials* **2005**, *26*, 5864.
[114] X. Tao, W. B. Kyle, Z. A. Mohammad, D. Dennis, Z. Weixin, J. Y. James, A. Anthony, *Biofabrication* **2013**, *5*, 015001.
[115] J. H. Y. Chung, S. Naficy, Z. Yue, R. Kapsa, A. Quigley, S. E. Moulton, G. G. Wallace, *Biomater. Sci.* **2013**, *1*, 763.
[116] M. Xu, X. Wang, Y. Yan, R. Yao, Y. Ge, *Biomaterials* **2010**, *31*, 3868.
[117] a) S. E. Bakarich, M. I. H. Panhuis, S. Beirne, G. G. Wallace, G. M. Spinks, *J. Mater. Chem. B* **2013**, *1*, 4939; b) S. Hong, D. Sycks, H. F. Chan, S. Lin, G. P. Lopez, F. Guilak, K. W. Leong, X. Zhao, *Adv. Mater.* **2015**, *27*, 4035; c) A. Skardal, J. Zhang, G. D. Prestwich, *Biomaterials* **2010**, *31*, 6173.
[118] W. Kim, G. H. Kim, *Chem. Eng. J.* **2018**, *334*, 2308.
[119] H. F. Chan, R. Zhao, G. A. Parada, H. Meng, K. W. Leong, L. G. Griffith, X. Zhao, *Proc. Natl. Acad. Sci. USA* **2018**, *115*, 7503.
[120] N. K. Abigail, K. Megha, A. P. Courtney, D. B. Daniel, D. Mehmet, W. Lin, L. C. Rebecca, *Biofabrication* **2016**, *8*, 035011.

[121] J. Yu, S. Peng, D. Luo, J. C. March, *Biotechnol. Bioeng.* **2012**, *109*, 2173.
[122] K.-Y. Shim, D. Lee, J. Han, N.-T. Nguyen, S. Park, J. H. Sung, *Biomed. Microdevices* **2017**, *19*, 37.
[123] K. Molly, M. V. Woestyne, W. Verstraete, *Appl. Microbiol. Biotecnol.* **1993**, *39*, 254.
[124] J. E. Koper, L. M. Loonen, J. M. Wells, A. D. Troise, E. Capuano, V. Fogliano, *Mol. Nutr. Food Res.* **2019**, *63*, 1800722.
[125] P. Van den Abbeele, C. Belzer, M. Goossens, M. Kleerebezem, W. M. De Vos, O. Thas, R. De Weirdt, F.-M. Kerckhof, T. Van de Wiele, *ISME J.* **2013**, *7*, 949.
[126] P. Van den Abbeele, C. Grootaert, M. Marzorati, S. Possemiers, W. Verstraete, P. Gérard, S. Rabot, A. Bruneau, S. El Aidy, M. Derrien, *Appl. Environ. Microbiol.* **2010**, *76*, 5237.
[127] M. Marzorati, B. Vanhoecke, T. De Ryck, M. S. Sadabad, I. Pinheiro, S. Possemiers, P. Van den Abbeele, L. Derycke, M. Bracke, J. Pieters, *BMC Microbiol.* **2014**, *14*, 133.
[128] a) E. Barroso, C. Cueva, C. Peláez, M. C. Martínez-Cuesta, T. Requena, *LWT–Food Sci. Technol.* **2015**, *61*, 283; b) C. Cueva, A. Jiménez-Girón, I. Muñoz-González, A. Esteban-Fernández, I. Gil-Sánchez, M. Dueñas, P. J. Martín-Álvarez, M. Pozo-Bayón, B. Bartolomé, M. Moreno-Arribas, *Food Res. Int.* **2015**, *72*, 149; c) A. Tamargo, C. Cueva, L. Laguna, M. V. Moreno-Arribas, L. A. Munoz, *J. Funct. Foods* **2018**, *50*, 104; d) I. Gil-Sánchez, C. Cueva, M. Sanz-Buenhombre, A. Guadarrama, M. V. Moreno-Arribas, B. Bartolomé, *J. Food Compos. Anal.* **2018**, *68*, 41.
[129] C. Cueva, I. Gil-Sánchez, A. Tamargo, B. Miralles, J. Crespo, B. Bartolomé, M. V. Moreno-Arribas, *Food Chem. Toxicol.* **2019**, *132*, 110657.
[130] M. Minekus, P. Marteau, R. Havenaar, J. H. J. Huis in 't Veld, *ATLA, Altern. Lab. Anim.* **1995**, *23*, 197.
[131] M. Larsson, M. Minekus, R. Havenaar, *J. Sci. Food Agric.* **1997**, *74*, 99.
[132] D. M. Ribnicky, D. E. Roopchand, A. Oren, M. Grace, A. Poulev, M. A. Lila, R. Havenaar, I. Raskin, *Food Chem.* **2014**, *142*, 349.
[133] M. Verwei, A. P. Freidig, R. Havenaar, J. P. Groten, *J. Nutr.* **2006**, *136*, 3074.
[134] N. M. Anson, R. Havenaar, A. Bast, G. R. Haenen, *J. Cereal Sci.* **2010**, *51*, 110.
[135] M. Verwei, M. Minekus, E. Zeijdner, R. Schilderink, R. Havenaar, *Int. J. Pharm.* **2016**, *498*, 178.
[136] M. Minekus, M. Smeets-Peeters, A. Bernalier, S. Marol-Bonnin, R. Havenaar, P. Marteau, M. Alric, G. Fonty, *Appl. Microbiol. Biotechnol.* **1999**, *53*, 108.
[137] A. Maathuis, A. Hoffman, A. Evans, L. Sanders, K. Venema, *J. Am. Coll. Nutr.* **2009**, *28*, 657.
[138] S. G. Sáyago-Ayerdi, V. M. Zamora-Gasga, K. Venema, *Food Res. Int.* **2019**, *118*, 89.
[139] C. B. de Souza, G. Roeselers, F. Troost, D. Jonkers, M. Koenen, K. Venema, *J. Funct. Foods* **2014**, *11*, 210.
[140] a) M. Cuevas-Tena, A. Alegria, M. J. Lagarda, K. Venema, *J. Funct. Foods* **2019**, *54*, 164; b) M. Aguirre, D. M. Jonkers, F. J. Troost, G. Roeselers, K. Venema, *PLoS One* **2014**, *9*, e113864.
[141] M. H. Van Nuenen, K. Venema, J. C. Van Der Woude, E. J. Kuipers, *Dig. Dis. Sci.* **2004**, *49*, 485.
[142] M. H. van Nuenen, R. A. de Ligt, R. P. Doornbos, J. C. van der Woude, E. J. Kuipers, K. Venema, *FEMS Immunol. Med. Microbiol.* **2005**, *45*, 183.
[143] E. C. H. H. Wessels, G. Schaafsma, J. van der Greef, J. J. M. van de Sandt, J. H. J. van Nesselrooij, K. Venema, R.-J. A. N. Lamers, *J. Nutr.* **2003**, *133*, 3080.
[144] K. Stamatopoulos, H. K. Batchelor, M. J. Simmons, *Eur. J. Pharm. Biopharm.* **2016**, *108*, 9.
[145] M. Wiese, B. Khakimov, S. Nielsen, H. Sørensen, F. van den Berg, D. S. Nielsen, *PeerJ* **2018**, *6*, e4268.
[146] T. Cieplak, M. Wiese, S. Nielsen, T. Van de Wiele, F. van den Berg, D. S. Nielsen, *FEMS Microbiol. Lett.* **2018**, *365*, fny231.
[147] F. Kong, R. P. Singh, *J. Food Sci.* **2010**, *75*, E627.
[148] a) M. Minekus, M. Alminger, P. Alvito, S. Ballance, T. Bohn, C. Bourlieu, F. Carriere, R. Boutrou, M. Corredig, D. Dupont, *Food Funct.* **2014**, *5*, 1113; b) O. Ménard, C. Bourlieu, S. C. s. De Oliveira, N. Dellarosa, L. Laghi, F. Carrière, F. Capozzi, D. Dupont, A. Deglaire, *Food Chem.* **2018**, *240*, 338; c) L. Egger, O. Ménard, C. Delgado-Andrade, P. Alvito, R. Assunção, S. Balance, R. Barberá, A. Brodkorb, T. Cattenoz, A. Clemente, *Food Res. Int.* **2016**, *88*, 217.
[149] K. W. Stapleton, E. Guentsch, M. K. Hoskinson, W. H. Finlay, *J. Aerosol Sci.* **2000**, *31*, 739.
[150] a) R. G. Shah, T. Girardi, G. Merz, P. Necaise, C. M. Salafia, *Placenta* **2017**, *57*, 9; b) K. M. Tse, P. Chiu, H. P. Lee, P. Ho, *J. Biomech.* **2011**, *44*, 827.
[151] a) S. M. Harrison, P. W. Cleary, M. D. Sinnott, *Food Funct.* **2018**, *9*, 3202; b) L. Fullard, W. Lammers, G. C. Wake, M. J. Ferrua, *Food Funct.* **2014**, *5*, 2731; c) M. J. Ferrua, R. P. Singh, in *New Advances in Gastrointestinal Motility Research* (Eds: L. K. Cheng, A. J. Pullan, G. Farrugia), Springer, Dordrecht, Netherlands **2013**, p. 243 (https://doi.org/10.1007/978-94-007-6561-0_13); d) M. J. Ferrua, R. P. Singh, *J. Food Sci.* **2010**, *75*, R151; e) C. de Loubens, R. G. Lentle, R. J. Love, C. Hulls, P. W. M. Janssen, *J. R. Soc., Interface* **2013**, *10*, 20130027; f) A. Pal, J. G. Brasseur, B. Abrahamsson, *J. Biomech.* **2007**, *40*, 1202.
[152] a) Y. Wang, J. G. Brasseur, G. G. Banco, A. G. Webb, A. C. Ailiani, T. Neuberger, *Philos. Trans. R. Soc., A* **2010**, *368*, 2863; b) R. J. Love, R. G. Lentle, P. Asvarujanon, Y. Hemar, K. J. Stafford, *Food Dig.* **2013**, *4*, 26.
[153] B. Jeffrey, H. S. Udaykumar, K. S. Schulze, *Am. J. Physiol.: Gastrointest. Liver Physiol.* **2003**, *285*, G907.
[154] A. Alexiadis, K. Stamatopoulos, W. Wen, H. Batchelor, S. Bakalis, M. Barigou, M. Simmons, *Comput. Biol. Med.* **2017**, *81*, 188.
[155] M. N. Read, A. J. Holmes, *Front. Immunol.* **2017**, *8*, 538.
[156] J. J. Faith, N. P. McNulty, F. E. Rey, J. I. Gordon, *Science* **2011**, *333*, 101.
[157] K. Z. Coyte, J. Schluter, K. R. Foster, *Science* **2015**, *350*, 663.
[158] A. J. Holmes, Y. V. Chew, F. Colakoglu, J. B. Cliff, E. Klaassens, M. N. Read, S. M. Solon-Biet, A. C. McMahon, V. C. Cogger, K. Ruohonen, *Cell Metab.* **2017**, *25*, 140.
[159] I. Thiele, B. Ø. Palsson, *Nat. Protoc.* **2010**, *5*, 93.
[160] S. Magnúsdóttir, A. Heinken, L. Kutt, D. A. Ravcheev, E. Bauer, A. Noronha, K. Greenhalgh, C. Jäger, J. Baginska, P. Wilmes, *Nat. Biotechnol.* **2017**, *35*, 81.
[161] F. Santos, J. Boele, B. Teusink, *Methods Enzymol.* **2011**, *500*, 509.
[162] D. Gilbert, M. Heiner, Y. Jayaweera, C. Rohr, *Briefings Bioinf.* **2017**, *1*, https://doi.org/10.1093/bib/bbx096.
[163] M. N. Read, K. Alden, L. M. Rose, J. Timmis, *J. R. Soc., Interface* **2016**, *13*, 20160543.
[164] a) J. F. Petrosino, *Genome Med.* **2018**, *10*, 12; b) P. C. Kashyap, N. Chia, H. Nelson, E. Segal, E. Elinav, *Mayo Clin. Proc.* **2017**, *92*, 1855.
[165] M. N. Read, K. Alden, J. Timmis, P. S. Andrews, *Briefings Bioinf.* **2018**, *1*, https://doi.org/10.1093/bib/bby092.